2013

Development of a reactor with optical access for in-situ analysis of fast pyrolysis

Willem Lubberden
Iowa State University

Development of a reactor with optical access for in-situ analysis of fast pyrolysis

by

Willem Michael Lubberden

A thesis submitted to the graduate faculty

in partial fulfillment of the requirements for the degree of

MASTER OF SCIENCE

Major: Mechanical Engineering

Program of Study Committee:
Terrence Meyer, Major Professor
Robert Brown
Brent Shanks

Iowa State University

Ames, Iowa

2013

TABLE OF CONTENTS

LIST OF FIGURES

ACKNOWLEDGEMENT

Anytime a long research project is completed many people are involved from start to finish. I would like to thank Dr. Meyer for giving me the opportunity to work in his lab, and for providing guidance for the duration of this project. I also appreciate Dr. Brown and Dr. Shanks for being on my committee. I would also like to thank lab mates Jordan Tiarks, Ben Halls, James Michael and Chloe Dedic for helping with experimental set-ups and giving great advice. From the biorenewable laboratory Patrick Johnston and Cuong Ho Kim were very helpful with experimentation expertise in this field. I'm grateful for my colleague Nandith Chandy for helping me with many aspects of my project, from building test sections in the lab to finding references. I would also like to acknowledge Deb Schroeder, Carol Knutson, and Amy Carver for their administrative support, and I thank to Jim Dautremont for having all the little parts on hand to help me with my research. Thank you to my parents for their unwavering support throughout my educational career. I would finally like to recognize my incredible wife Chelsea, who never stopped believing in me when at times I did not think I was cut out for graduate school, and I am forever grateful for that. I can't wait to continue on our journey together and will never forget the immense encouragement and love you gave me.

ABSTRACT

A pyrolysis reactor with optical access was developed to study the *in-situ* reactions taking place during the first stages of fast pyrolysis. All aspects of the reactor are documented, including sample insertion, temperature profiling, and species measurements. Analytical instruments including a gas chromatograph-flame ionization detector (GC/FID) and a Fourier transform infrared spectrometer (FTIR) were used in the experiments. In the case of the FTIR, a commercial instrument was modified to allow *in situ* analysis and to enable sufficient sensitivity for time-resolved measurements during the reaction. Cellulose and Lignin were pyrolyzed, and qualitative identification of the main products was gained from the chromatogram with the FTIR as a function of residence time in the reactor. Also, hybrid femtosecond/picosecond coherent anti-Stokes Raman scattering (fs/ps CARS) was applied to study phenol and 2,2'-biphenol demonstrating the capability of identifying biomass products using a non-invasive, spatio-temporally resolved *in-situ* technique. Finally, the optical access in the reaction chamber allowed direct time-resolved visualization of the pryrolysis process within the reaction zone. The data collected in this work illustrate that the implementation of *in-situ* diagnostic techniques can potentially provide new information on spatio-temporally dependent physicochemical processes that are relevant to biomass conversion.

CHAPTER 1. INTRODUCTION

1.1 Motivation

The world is facing a crossroad when it comes to producing efficient clean energy in a sustainable manner. As the population continues to rise, limited resources are extracted at an alarming rate to accommodate electric power generation and transportation, among other basic needs. Also, extracting fossil fuel resources such as crude oil and natural gas are becoming more energy intensive. The price of oil is predicted to rise, with some projections estimating oil prices to reach over $200/barrel by 2040 [1]. Beyond economic considerations, the increase of green house gas emissions (e.g., CO_2) being released is also a major concern for the global climate. An alternative to the current approach is to use biomass feedstocks grown through the process of photosynthesis to produce chemicals and fuel. Plants convert carbon dioxide and sunlight into food to grow and release oxygen as a byproduct, providing a carbon sink for conversion technologies. The fast growing cycle, availability, and ease of transportation presents a viable avenue to produce commodities.

All of these factors present the need to develop effective thermochemical technologies to convert biomass into power, chemicals, and fuels. The United States government has set a goal through the Energy Independence and Security Act of 2007 which expands the setpoint to bio-based fuels to 36 billion gallons annually produced by 2022 [2]. Three major thermochemical conversion methods are gasification, combustion, and pyrolysis. Fast pyrolysis in particular has been recently emerging as a techno-economically viable biomass upgrading technology. Fast pyrolysis is a relatively

new technology where fundamental research did not start taking place until the late 1970s. The first reactor completed in 1979 at the University of Waterloo was used to determine how to achieve maximum bio-oil production from aspen-poplar wood [3]. Many factors were identified that affect pyrolysis yield, including vapor residence time, heat transfer, and temperature, which continue to be characterized today. In order to understand these variables in more detail, experimental avenues must also advance to understand conversion processes. Due to the complex molecular structure of plant material, chemical reactions and pathways in fast pyrolysis are also difficult to characterize. This presents motivation to develop a pyrolysis instrument with the capabilities of applying many different techniques into one reactor to analyze the fundamental pathways of biomass fast pyrolysis.

This thesis overviews the development of a bench scale pyrolysis reactor to analyze reactions *in situ*, with *in situ* translating literally to "in-position", meaning in this context as inspecting the reaction as it is happening. The novelty of this work lies in the fact that there has been little work in the field of fast pyrolysis research on the inspection of the reaction providing high temporal and spatial resolution. Often, the experimental work is conducted under varying conditions to inspect how the maximum yield of bio-crude can be achieved without considering fundamental reactions taking place. Because there is relatively little prior work in this area, a number of experimental techniques and instruments are surveyed in this work to exemplify the capabilities of the optically accessible pyrolysis instrument, including direct high-speed imaging, Fourier transform infrared (FTIR) spectroscopy, and coherent anti-stokes Raman scattering

(CARS). In addition, *ex situ* characterization of the product stream was conducted using a gas chromatograph-flame ionization detector (GC/FID) to validate the pyrolysis process. Each of these experimental techniques provide unique capabilities towards achieving the goal of addressing fundamental questions regarding physicochemical processes occurring during fast pyrolysis.

1.2 Objective

The objective of this project is to design a bench scale optically accessible fast pyrolysis instrument with the capabilities of applying spectroscopic techniques to effectively characterize the pyrolysis reaction process. The essential design parameters include temperature, sample insertion, and residence time to effectively study *in-situ* pyrolysis. The second portion is to demonstrate the techniques that can be used in conjunction with the pyrolysis cell successfully, including CARS, FTIR, and GC-FID. All of these techniques in combination can be used to gain greater insight into how biomass decomposes and to address fundamental questions about the fast pyrolysis process.

CHAPTER 2. LITERATURE REVIEW

2.1 Characterization and Composition of Biomass

Biomass is generally defined as organic matter of recent biological origin [4]. The emphasis is on "recent" being distinguishable from more well known organic material such as coal and petroleum that take millions of years to form. Biomass has the ability to be grown in quick growing cycles, utilizing CO_2 during the growth of the plant. Thus, the term biorenewable resource has been used to describe the use and implementation of biomass to produce power, chemicals, and fuels through thermochemical conversion techniques. Many feedstocks have been used with wood being the oldest to be used by man for heat through combustion. Recently, switch grass, corn stover, and algae have been used more readily to produce commodities. A more precise classification can be made for lignocellulosic biomass, which excludes the starch and sugar crops such as corn, soybeans, and sugarcane.

The chemistry behind plant material is complex with no two plant species have the same chemical structure. Lignocellulosic biomass consists of a matrix of cellulose, hemicellulose, and lignin. Each of these components play a major role the structure of the plant[4]. Figure 2.1 breaks down how one can visualize how constituents fit together within the cell wall of a plant. The typical range of wt. % of cellulose, hemicellulose, and lignin are 20-40, 40-60, and 10-25, respectively [5]. Many groups have studied these three components without considering the entire biomass as a whole since the main portion of the plant does consist of these three polymers [6-8]. Through knowledge of

how these three components decompose during pyrolysis, many new insights can be drawn about the decomposition of biomass and interactions between its constituents.

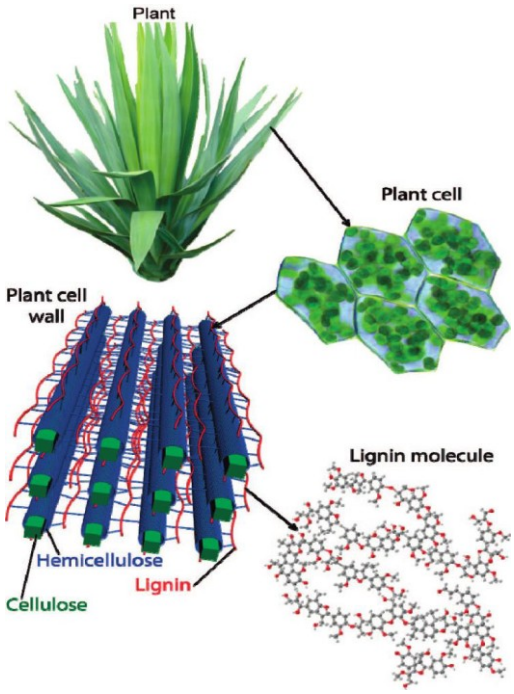

Figure 2.1: Structure of lignocellulose material directly obtained from [9].

2.1.1 Cellulose

Cellulose is a polysaccharide which consists of long chain of glucose molecules linked by glycosidic bonds [10]. Cellulose molecules have strong affinity for hydrogen bonding which forms bundles called microfibrils. These structures are highly ordered, which gives cellulose high tensile strength and insolubility in most solvents [11]. If these bonds are broken up into individual components, the sugar monomers can be used by microorganisms for fermentation. Understanding cellulose pyrolysis is important because it is common in lignocellulosic materials, with wood consisting of approximately of 40-45% in most species.

2.1.2 Hemicellulose

Hemicellulose is considered a heteropolysaccharide consisting of many monomeric compounds. These monomers are hexoses and pentoses and small amounts of uronic acids including D-glucose, D-mannose, D-xylose, L-arabinose, D-glucuronic acid, 4-O-methyl-D-glucuronic acid, and glacturonic acid [11]. Hemicellulose is more amorphous, containing a lower degree of polymerization than cellulose, thus making it more susceptible to hydrolyze into sugars. Since it takes some expertise to extract hemicellulose from biomass, it is common to use xylan from major chemical distributors for experimental purposes. Xylans are common in hard wood hemicelluloses, whereas softwoods generally have more mannose and galactose units [4].

2.1.3 Lignin

Lignin is a non-carbohydrate phenylpropane-based polymer consisting of three monomers including coniferyl alcohol, sinapyl alcohol, and coumaryl alcohol. These alcohols all contain benzene rings with functional groups including phenolic, hydroxyl, methoxy, and aldehyde groups leading to chemical reactions that form many products common in lignin pyrolysis. Its main purpose for the plant is to protect the cell wall from biological attack, thus making it insoluble to solvents and a challenge in biofuel conversion [12]. Hence, lignin pyrolysis can present important challenges in the future of biomass conversion systems. Lignin is classified by the way it is extracted, since chemical properties are often modified in the process. Common classifications are sulfate, organosolv, and enzymatic hydrolysis lignins, which all are methods for separating lignin from the rest of the plant.

2.2 Biomass Fast Pyrolysis

2.2.1 Introduction

Pyrolysis is the rapid heating of a feedstock to a temperature of 300 to 600° C in a low-oxygen environment. Slow and fast pyrolysis refer to the heating rates applied to the biomass, with slow pyrolysis producing charcoal (if the biomass is wood), whereas in fast pyrolysis the condensable gases are of interest. Fast pyrolysis consists of heating biomass at high heating rates of thousands of degrees per second and quenching the products in short residence times (1-3 s). These high heating rates produce condensable and non-condensable vapors and bio-char in varying amounts depending on the feedstock. The exact mechanism on how this depolymerization of the biomass takes place is still under debate with two theories being proposed. The main goal of fast pyrolysis is to maximize the condensable yield of the products to form bio-oil. Bio-oil or bio-crude is used for co-firing in boilers, refined to make fuels, or modified to be used for the chemical industry. Many studies have been conducted to identify optimal conditions to produce the most liquid product which will be described in more detail in a later section. Many reactors have also been developed to optimize heat transfer to particles and condense the vapor in the most efficient way. The fundamental aspects of fast pyrolysis are still being pursued with the mechanisms leading to certain unwanted products being poorly understood. The rest of this section will cover the reaction pathways, bio-oil characteristics, reactor designs, and challenges moving forward.

2.2.2 Reaction Pathways and Mechanisms

During fast pyrolysis biomass can decompose in a variety of ways with the end products depending on many factors associated with the reactor and sample. The

variable nature of the reaction kinetics makes it difficult to create encompassing models that are consistent. The first model proposed by Broido and Nelson depicts cellulose pyrolysis as two single step reactions found through a thermogravimetric study [13]. They concluded at temperatures lower than 250°C cellulose was converted into char and low molecular weight compounds. At temperatures above 280°C another competing reaction led to tar formation. A slight modification by Shafizadeh et. al concluded that cellulose transitions into a anhydro fragment referred to as "active cellulose" before degrading into char, tar, and gases [14]. The condensable gas portion also contains the water content of the biomass; thus, as the reaction proceeds secondary cracking occurs and other gases can be formed. Each component of biomass has different thermal degradation properties, which results in unique product distributions for different processes. There has been significant work in trying to define this model better by characterizing the primary and secondary reactions of cellulose by Patwardhan et al. [15]. They compared the product distribution from cellulose in a micro-pyrolyzer with short residence times <1 s and a fluidized bed reactor >1 s and found polymerization of levoglucosan played a major role in primary reaction products. Therefore, an understanding of the product evolution during fast pyrolysis would help address long-standing questions about the source of certain species found in typical bio-oils.

With regard to initial decomposition, there are also differing viewpoints on how the liquid is physically ejected from the biomass and what mechanism forms higher molecular weight compounds. Teixeira et al. proposes a "reactive boiling ejection" approach with aerosols being driven out from the particles and directly forced into

organic liquid particles [16]. Also, Dauenhauer et al. imaged cellulose on an Al_2O_3 catalytic plate and observed the formation of intermediate liquid before boiling into the vapor phase [17]. These decomposition studies are controversial as the heating is only applied on one side of the particle rather than encompassing the entire sample simulating pyrolysis conditions in a reactor. Another hypothesis is the sample decomposes into a gas first with secondary reactions nucleating and polymerizing into the compounds that are found in the bio-oil. More research needs to be done in this area to fully understand and answer these fundamental questions by using new techniques to simulate high heating rates involved with fast pyrolysis.

2.2.3 Bio-Oil Characteristics

Bio-oil is the valued product that is derived from fast pyrolysis when the volatiles are quickly quenched and condensed into the liquid state. It is a dark colored viscous liquid with many unique properties depending on the feedstock and how it was produced. Bio-oil does have some general characteristics that make it advantageous over other conversion technologies, including ease of transportation, storage, and reactor feeding [10]. In Table 2.1 many important properties are shown of a typical bio-oil derived from wood. It should be noted that these properties fluctuate with great regularity depending on the feedstock and process parameters in place.

Table 2.1: Bio-oil properties from wood taken from Bridgwater [18]

Physical Property	Typical Value
Moisture Content	25%
pH	2.5
Specific gravity	1.20
Elemental analysis C	56%

Table 2.1 continued

H	6%
O	38%
N	0-0.1%
HHV	17 MJ/kg
Viscosity (40C and 25% water)	40-100 cp

Characteristics
Liquid fuel
Ready for substitution for conventional fuels in many stationary applications such as boilers, engines,
Heating value of 17 MJ/kg at 25% wt. water, is about 40% that of fuel oil/diesel
Does not mix with hydrocarbon fuels
Not as stable as fossil fuels
Quality needs definition for each application

2.2.4 Reactor types

Many reactors have been built to pyrolyze biomass quickly and effectively to attain the large bio-oil yield. In most cases the size of the reactor depends on the amount of biomass that can be fed over a specified time. Scalability is an important factor in reactors, which are often characterized as bench, pilot, or industrial scale reactors in order of increasing size and/or mass flow. There are many design parameters that go into making an effective fast pyrolyzer, with major factors including residence time, heat transfer to the biomass, and the feeding system. Challenges arise when trying to insert the feedstock into the reactor due to particle size, flow ability, and variance of the biomass without affecting reactor performance. The most common type is a fluidized bed reactor which utilizes a large bed of sand with hot gas imposing high heat transfer rate to the biomass particles. These can be scaled to large sizes easily, which is important for going from a pilot to an industrial plant. Some other reactors that are used

are ablative, entrained flow, and vacuum pyrolyzers. Ablative uses a hot spinning disk that causes biomass to thermally decompose through conduction. There are many reviews that cover each technology which describe the advantages and disadvantages of each type and how it is used for each feedstock [19-21].

2.2.5 Challenges and Future

There are many challenging aspects of fast pyrolysis that need to be resolved to make it an economical and viable thermochemical conversion technique and competitive in today's market. The complexity of the feedstocks and the complicated nature of reactions that take place under short time durations have proven to be major obstacles in moving forward. Mettler et al. identified ten items of interest that need to be studied more in depth to commercialize biomass fast pyrolysis [22]. Two of the challenges regarding experimental techniques are to visualize/characterize biomass chemistry and validate particle models to improve the bio-oil quality overall. If the chemistry can be clarified to a high degree regarding how biomass breaks down in a pyrolysis environment,t the overall efficiency and yields can potentially be optimized. In addition, there also has been work done to introduce catalysts into fast pyrolysis reactors to attain the desired products. Srinivasan et al. added zeolite catalysts to promote hydrocarbon formation through fast pyrolysis [23]. As the demand for alternative fuels continues to rise, there will be an increasing need to investigate fast pyrolysis reactions. Many approaches are being suggested to increase the overall efficiency to make a profitable end product and eventually replace fossil derived oil.

2.3 Fourier Transform Infrared Spectroscopy

2.3.1 FTIR fundamentals

FTIR Spectroscopy is an analytical technique that elucidates information on the molecular structure of the sample. The spectrum obtained from FTIR is typically an absorbance versus wavenumber displaying peaks corresponding to various molecular bonds. A requirement to observe infrared absorption is there must be a net change in the dipole moment of the functional group or molecule of interest [24]. The frequency variation of absorbance bands is based on different energy needed to probe the transitions in the molecular bonds. The infrared region is generally defined from 14,000-4 cm-1, but many studies are only interested in the mid-infrared (4000-400 cm-1) since this is where the most fundamental vibrations occur. Many organic samples contain bonds that exhibit activity in the infrared, so it is used often for identification and concentration measurements in bio-chemistry.

FTIR Spectroscopy is named after Joseph Fourier, who is responsible for the development of the mathematical transform that takes any function and forms it into a superposition of sine and cosine waves. Through this operation it is possible to calculate the absorbance for a given wavenumber without scanning through each individual frequency as is done with other instrumentation. This is possible by the use of an interferometer which consists of a beam splitter and a moving mirror to which one scan corresponds to the cycle motion of the mirror. This movement creates an interferogram based on the optical path difference between the IR beam of all the wavelengths. The absorbance spectrum is calculated through the use of the Fourier Transform while

subtracting out the background [25]. Figure 2.2 shows how the FTIR internal components are placed together to form a spectrum.

The detector is chosen based on the needs of the user such as response time,

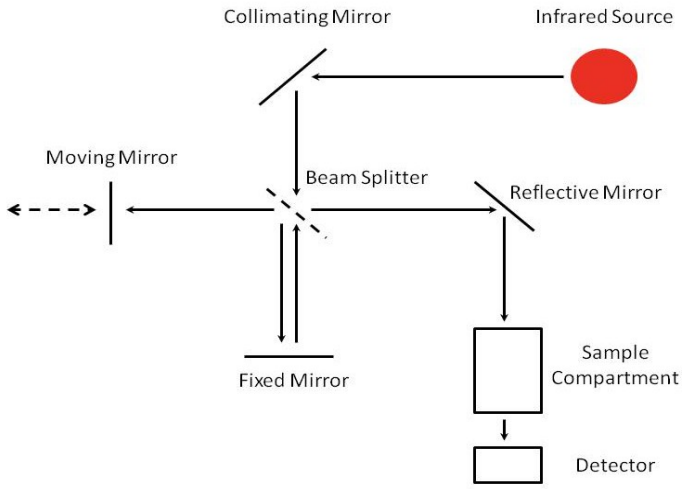

Figure 2.2: Internal components of Fourier transform infrared instrumentation

sensitivity, and wavenumber range. Some of the most common types of detectors are triglycine sulfite (TGS) and mercury cadmium telluride (MCT). The beam splitter is also varied based on what part of the infrared spectrum (near, mid or far) is being investigated.

With all instrumentation there are always advantages and disadvantages associated with its functionality. The advantages consist of fast sampling, sensitivity, and the varied kinds of samples that can be tested [25]. All three phases of matter can be used with FTIR spectroscopy, with sample preparation methods differing depending on the application. Some disadvantages are that water vapor and CO_2 absorbs heavily in the infrared causing distorting results at times. Therefore, the sample chamber and where the beam is routed must be purged to minimize these affects. Also, trying to distinguish

the molecular structure of a mixture can make the spectra very complicated and difficult to identify individual species. However, with the right tools and knowledge, spectroscopists can interpret even complex spectra to attain structure and chemistry information.

2.3.2 Infrared Spectra Interpretation

Table 2.2: Major functional groups of cellulose, hemicellulose and lignin [8].

Wavenumber (cm^{-1})	**Functional groups**	**Compounds**
3600-3000	OH stretching	Acid, methanol
2860-2970	C–H_n stretching	Alkyl, aliphatic, aromatic
1700-1730		
1510-1560	C=O stretching	Ketone and carbonyl
1632	C=C	Benzene stretching ring
1613, 1450	C=C stretching	Aromatic skeletal mode
1470-1430	O–CH_3	Methoxy–O–CH_3
1440-1400	OH bending	Acid
1402	CH bending	
1232	C–O–C stretching	Aryl-alkyl ether linkage
1215	C–O stretching	Phenol
1170,1082	C–O–C stretching vibration	Pyranose ring skeletal
1108	OH association	C–OH
1060	C–O stretching and C–O deformation	C–OH (ethanol)
900-700	C–H	Aromatic hydrogen
700-400	C–C stretching	

There are many techniques used to breakdown infrared spectra and interpret the chemistry of the sample. The observed attributes of a peak in the spectrum are broadness and wavenumber. The sharpness of a peak is often determined by area under the absorption response. Each peak represents a vibrational band that can be identified through reference spectra or process of elimination. Table 2.2 shows the major groups that can be identified for pure cellulose, hemicellulose, and lignin. Using this

knowledge, large functional groups can be ruled out if certain wavenumber ranges are not active. Coates breaks down how to interpret spectra by providing a step by step approach to identify bands in an unknown substance [24]. Important aspects are to understand what type of sample is being processed and break down the elements to certain regions to focus on so that an entire picture can be made of the major bonds. By following a simple procedure and using process of elimination major chemical structures can be identified from an infrared absorbance spectrum.

2.3.3 Thermal Decomposition studies of Biomass

The most common experimental method with infrared spectroscopy performed with biomass is thermo-gravimetric-FTIR (TG-FTIR). By knowing the heating rate, it is possible to identify the temperatures at which certain products are released from different samples. Moreover, the heating rate can be varied to determine if this has an impact on product formation. This method does not simulate fast pyrolysis as the heating rates are on the order of tens of degrees per minute. Yang et al. performed TG-FTIR of the three major components of lignocellulose and found which gas species were released at specific temperatures [8]. Major gas components including H_2, CO, CO_2, CH_4, C_2H_4, were also analyzed to determine the temperatures at which there respective concentrations increased the most for each sample. Coconut shell was analyzed in a high temperature DRIFT (Diffuse Reflectance Infrared Fourier Transform) cell with a heating rate of 83° C/min [26]. The data was used to determine the temperatures at which different bonding groups were released. Another thermal decomposition study performed by Bassilakis et al. tested a variety of feedstocks, including three types of

tobacco, wheat straw, and biomass model compounds [27]. Figure 2.3 displays a three dimensional plot of spectra collected in 30 second intervals of oriental tobacco with temperature increasing in the depth dimension from 150 to 900° C.

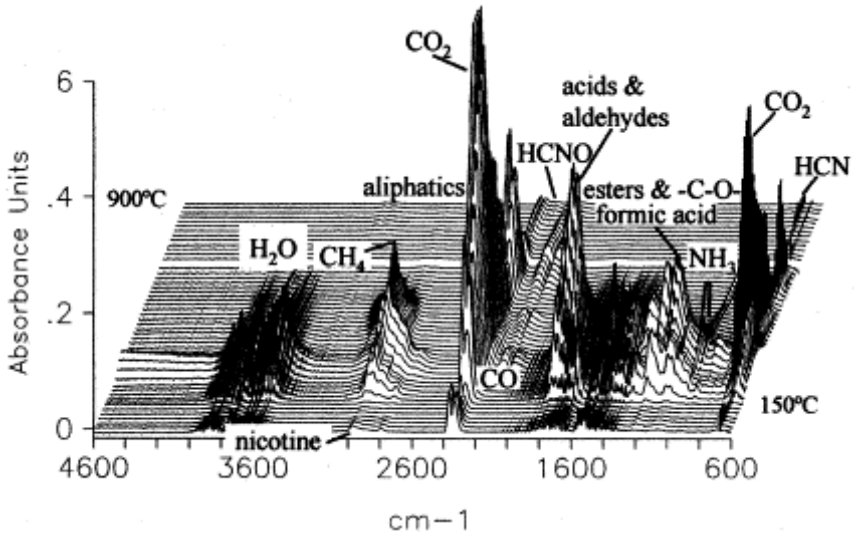

Figure 2.3: FTIR three dimensional plot of products of oriental tobacco [27]

These studies can be used to understand how and why biomass breaks down under certain heating conditions and to provide more information into the kinetics of the reactions. The limitations are that it does not model "fast" pyrolysis with low heating rates and the reactions are difficult to analyze. It is of interest, therefore, to implement FTIR in such a manner as to have high temporal resolution to capture the time dynamics of processes occurring for ~1-3 s.

2.3.4 Pyrolysis-FTIR

Fourier transform infrared spectroscopy is not typically implemented for *in situ* analysis, although it can be accomplished with custom modifications. Moreover, implementation with *in situ* TG-FTIR for biomass pyrolysis is not common. The work

done in these areas are often referred to as pyrolysis-FTIR (PFTIR) or rapid scan FTIR (RSFTIR). Feng et al. performed pyrolysis with a filament type micropyrolyzer encased in a cell to analyze the products released from lignite coal with different heating rates [28]. Another study employed the same micropyrolyzer with heating rates up 1000° C/s with corn cobs to build an analytical semi-empirical model based on corn cob pyrolysis [29]. The IR beam was located 3 mm above the sample to ascertain information on reaction kinetics in the pyrolysis process. Li et al. developed a technique that rapidly heats cellulose and sweeps the gases into a long path gas cell by a FTIR varying the heating rates and residence times [30]. The residence times were varied from 0.03 to 0.12 seconds to attempt to separate the primary and secondary reactions while controlling downstream temperature of the sample. The disadvantage of this approach is that functional groups of individual molecules can be determined, but identification of individual species is more difficult. PFTIR provides information that TG-FTIR cannot by applying much higher heating rates while probing a volume that is very close to the sample (neglecting assumptions regarding primary or secondary reactions). Hence, it is of interest to implement PFTIR to examine the initial reactions under fast pyrolysis conditions.

2.4 Coherent Anti-Stokes Raman Scattering

2.4.1 Fundamentals

Coherent anti-Stokes Raman scattering (CARS) spectroscopy is a nonlinear optical diagnostic technique used to measure temperature and species concentration in reacting flows. This technique is most useful in highly reactive or turbulent

environments where the use of physical probes is either difficult to implement or would disrupt the dynamics of the system. CARS offers high spatial resolution, and the coherent, laser-like signal generated is orders of magnitude greater than traditional Raman spontaneous emission. Traditionally, CARS is performed using a nanosecond laser source, but the development of ultrafast laser pulses (picosecond and femtosecond) has made this technique more effective in recent years. One challenge associated with probing a particular molecule to make a CARS measurement is nonresonant interference, and picosecond laser sources allow temporal discrimination between resonant and nonresonant signals [30]. Femtosecond laser sources offer high repetition rates (1-10 kHz) and high peak powers (~10^{10} W), increasing the usefulness of the CARS technique [31].

Three separate laser pulses are used to probe the molecule of interest. The first pulse, referred to as the pump pulse, is used to raise the energy to a virtual state while the Stokes pulse sends the molecule down to the next eigenstate. These two pulses are used simultaneously to generate a molecular coherence, while the third pulse probes this coherence, generating the CARS signal. The beams must also be phase matched to ensure constructive buildup of the signal rather than destructively reducing the response. In one phase-matching configuration known as BOXCARS, the pump, Stokes, and probe beams are crossed at a focal point, generating CARS in a very small sample region to provide high spatial resolution [32]. After the focal volume, all beams are blocked except for the CARS signal, which is directed into a spectrometer and camera assembly. The spectral information within this coherent signal contains information regarding

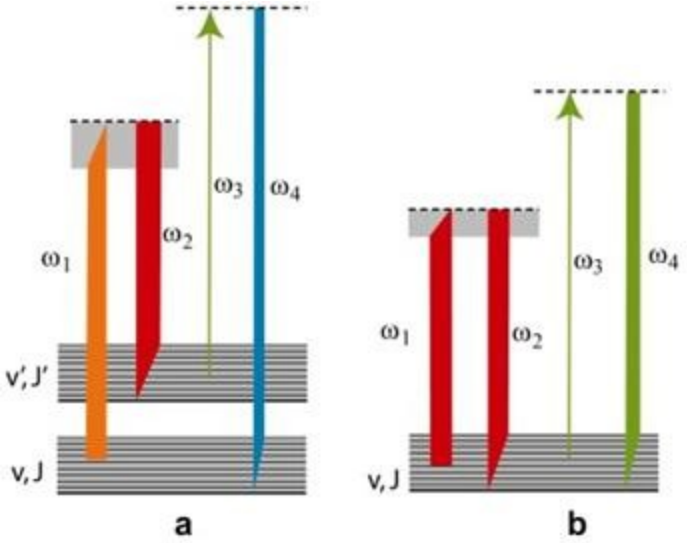

Figure 2.4 (a) Energy level diagrams for hybrid CARS (b) and pure rotational CARS used from Roy et al. [32].

temperature and species concentration. The energy diagram shown in Figure 2.4 demonstrates this phenomenon with the pump, Stokes, probe, and CARS beams corresponding to ω_1, ω_2, ω_3, ω_4, respectfully. The pump and Stokes pulses are selected based on the vibrational or rotational transitions of interest and are typically broadband, to excite many molecular species. Figure 2.4 (b) displays pure rotational CARS in which the pump and stokes pulses are the same wavelength. Rotational CARS differs from ro-vibrational CARS, which requires two lasers or an optical parametric oscillator to generate two colors of light. The rotational transitions are closely spaced in frequency, allowing the use of two degenerate pulses. Many different configurations of the basic CARS set-up have been used mainly by altering the shape and timing of the pulses to attain accurate temperature measurements from 300-3000 K and species concentrations, as reviewed extensively by Roy et al. [32].

2.4.2 Thermometry and Concentration Evaluation

Hybrid fs/ps CARS is a technique that has been extensively studied at Iowa State University, and it combines the benefits of picosecond and femtosecond CARS [33]. This technique is performed using a femtosecond laser source, providing the high peak power and repetition rates characteristic of femtosecond sources. Hybrid fs/ps CARS uses two broadband, 100-femtosecond pulses as the pump and Stokes beams, and pulse shaping is used to create a spectrally-narrowed, picosecond probe pulse that can be temporally delayed to suppress nonresonant background. This technique allows the detection of the molecular response in both the time and frequency domain. Temperature and species can be measured by comparing experimental data with theoretically modeled CARS data. Experimental and theoretical model comparisons of time and frequency domain information are shown by Stauffer et al. [in review] for N_2 in figure 2.5.

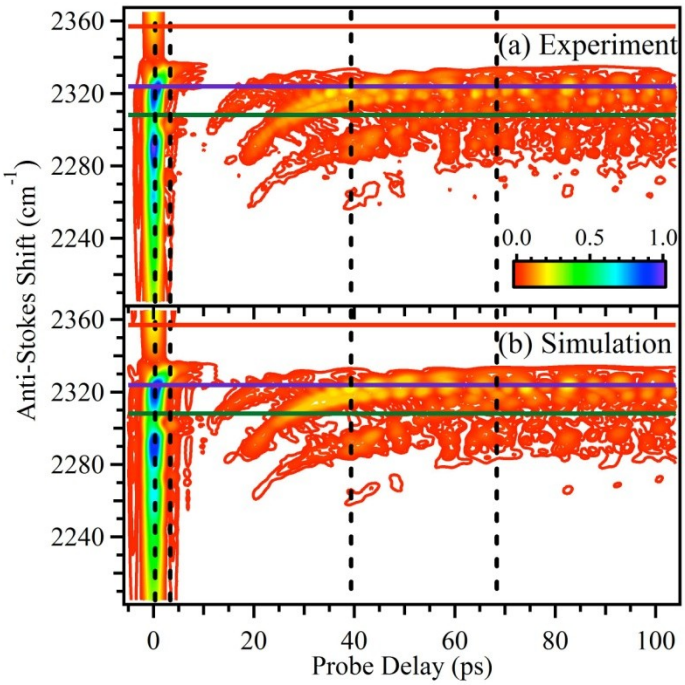

Figure 2.5: Time domain plot of experimental and simulated results of pure N_2 at 2370 K [in review].

Through modeling the molecular response, thermometry and species concentration of the sample can be obtained. Engel et al. demonstrated frequency-resolved concentration measurements of N_2 and CH_4 within a binary mixture by comparing the intensities of each transition at specific probe delays [34]. It is also possible to make concentration measurements in the time-domain, as performed by Richardson et al. [35] .

Miller et al. has implemented hybrid CARS of N_2 at one probe delay for thermometry [36]. To measure temperature, first a temperature dependent model must be developed for a specific molecule based on the Boltzmann distribution. For combustion experiments N_2 is typically used due to its high concentrations and inert

nature. A theoretical model is used to generate a library of spectra at various temperatures, and the experimental spectrum is compared to the library to find the best fit, providing the best fit temperature. A plot of experimental and theoretical N_2 CARS is shown in Figure 2.6, with open symbols and a solid line corresponding to the experimental results and the best-fit theoretical spectrum, respectively. This has proven to be an accurate method with an error of around 2.5% at combustion temperatures by Miller et. al [37].

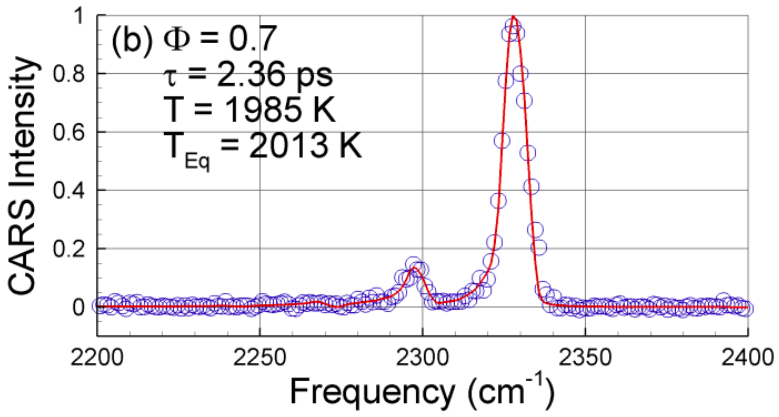

Figure 2.6: Frequency response of N_2 with a probe time delay of 2.36 ps [36].

2.4.3 Raman and Infrared Spectroscopy Comparison

Raman spectroscopy is only active when the polarization or deflection of the electron can be changed by incident radiation. In contrast, infrared active transitions are induced only when there is a dipole moment that can be altered during the vibrational mode of the molecule of interest. This explains why diatomic molecules of the same atom are not IR-active like N_2 and O_2. The rule of mutual exclusion in spectroscopy states that in a symmetric molecule all normal modes cannot be Raman and IR active.

However, it is possible for both to be inactive for a given molecule. Based on this principle the best technique can be chosen for the application and what species are being probed.

2.5 Bench Scale Pyrolyzers

2.5.1 Introduction

Pyrolysis instruments come in many shapes and sizes and use a variety of techniques for sample insertion and heating. A common reactor type is an entrained flow reactor for analyzing biomass due to its simple design. While groups develop in house reactors for their own experimental needs, it can cause discrepancies in data based on experimental parameters and design. This creates a demand to develop standard small scale micro-pyrolyzers to analyze fundamental mechanisms and product distributions of biomass. The main design constraints consist of sample insertion, heating rates, and volatile exhaust. In most cases micro-pyrolyzers are attached to other instruments such as gas chromatographs, mass spectrometers, and flame ionization detectors for product identification. Three micro-pyrolyzers will be reviewed, including an isothermal furnace, curie point filament, and resistive heating.

2.5.2 Isothermal Furnace

An isothermal furnace micropyrolyzer consists of a metal or glass section with a heating element placed on the exterior of the sample section. The sample is injected or dropped into the hot pyrolyzer when it is set to the correct temperature. This insures a high temperature gradient to the sample in the range of 2000°C/s [38]. The temperature is monitored and connected to a controller to maintain a constant thermal environment. A carrier gas flows into the pyrolysis reaction zone and moves the elutes into the exit

injection port for detection from other instrumentation. Special design considerations must made to insure samples are inserted without introducing oxygen into the pyrolysis reaction zone and that the sample temperature is known to a high precision. In most cases the pyrolyzer is calibrated to accurately measure the temperature along the centerline of the sample chamber. One disadvantage is injecting solid samples can be difficult, but liquids and gases are easily analyzed through syringe injection.

2.5.3 Curie Point Filament

A Curie point filament micro-pyrolyzer consists of a ferromagnetic material which is placed close to the sample with wires wrapped around the outside. An current is applied to electrical wires inducing the material heating to the curie point temperature based on the material properties of the coil. This technique provides good reproducibility on the temperature and can be heated reach pyrolysis conditions in milliseconds. The sample is either placed right next to the coil or actually dipped on the coil itself.

2.5.4 Resistive Heating Filament

The resistive heating filament micro-pyrolyzer is a small metallic material (typically iron, nichrome, or platinum) connected to a power source. The metal is connected directly to an electrical power source without induction taking place. A computer feedback system is often used to monitor temperature due to resistance changes as the filament is heated. This is done for the greatest reproducibility of the temperature. Samples are often placed right on the filament itself, or it can be held in place with quartz wool if the sample is a powder. The advantage with resistive heating is that a range of temperatures can be used rather than a specific set point as with the

curie point technique. Ronnse et al. optimized the use of this micropyrolyzer design to attain consistent and repeatable results of cellulose pyrolysis [39].

2.5.5 Bench Scale Entrained Flow Reactors

Entrained flow reactors have been used readily for bench scale pyrolysis due to inherent ease of designing and process parameter control. The basic design consists of a feeding system, heated reaction zone, and either a quenching system or analytical instruments to process the pyrolizates. An inert carrier gas is used to purge oxygen out of the system and act as a medium to move products through the reactor. There have been several groups that have implemented this method to study chemistry of pyrolysis while varying parameters such as heating rates, feed stocks, and process temperatures. Dayton developed a laminar entrained flow reactor and characterized the fluid dynamics and temperature profile within the reaction zone to perform accurate kinetic studies with cellulose particles [40]. The heating system consisted of 4-zone ceramic furnace with residence times near 1 s. A unique attribute to a reactor used by Dupont et al. consisted of a sampling probe that could be moved to different heights in the reactor attaining different residence times [41]. Another reactor with a unique configuration built by Shuangning et al. used plasma heated argon for the process heat [42]. Heating rates near 10^4 K/s were achieved on average with this technique. A experiment performed by Visentin et al. was performed in a heated quartz tube reactor and was able to investigate disturbances in the aggregative flow of the feeder system [43]. These reactors are being used readily in fundamental pyrolysis research. It is of interest in this work to incorporate the features of these reactors in an optically accessible configuration.

2.6 Sample Identification Techniques

2.6.1 Gas Chromatography Introduction

Gas chromatography separates a gas mixture into individual components so they can be identified with a mass spectrometer or other analytical detectors. The individual components of a gas stream are sent through a small capillary tube and react with a stationary phase on the inside of the column. The components are separated and leave the capillary at different elution times so they can be identified individually. The residence times are based on carrier gas flow rate, stationary phase, column length, temperature program, and column diameter. These parameters are also used to identify the best column to be used for specific gas samples. The polarity of the stationary phase also greatly affects the usefulness of the column based on the compounds being analyzed. The column is placed in an oven which is often controlled with a temperature program so that the gas elution times are reasonable. Based on what gas is being analyzed, this program is often adjusted depending on the sample being tested.

2.6.2 Mass Spectroscopy Introduction

Mass Spectrometers are common analytical tools used to identify gas molecules in pyrolysis experiments often attached directly to the gas chromatograph. There are three main parts of the instrument that allow identification to take place. First, a filament source ionizes the molecules usually by removing an electron. This is done by a stream of electrons moving through the sample gas to create ions. Second, the ionized material is organized by passing through a magnetic field which deflects the ions based on the molecular mass. A quadrupole mass spectrometer uses 4 tubes to induce the magnetic field and effectively repel the cations and attract anions. The magnitude of

field is altered throughout the analysis to deflect different sized ions to the detector. The third item is the detector which quantifies the amount of ionized particles for a given mass-to-charge ratio (*m/z*). This is done by directing the ion towards a wall of electrons which neutralize it and then the void is filled. A current is measured as the void is filled by electrons and then current versus *m/z* can be plotted. All of these steps must take place in a vacuum with pressures near 10^{-7} torr so that these ions don't react and form other molecules. The data is compared to a mass spectral database so that the correct molecule can be identified. There is a base peak typically that corresponds to the atomic mass of the compound since most of the ions have a charge equal to one. Also, the other peaks in a mass spectrum correspond to the fragmentation of the base molecule into separate entities. This technique provides a pathway to identify species in a gas stream.

2.6.3 Flame Ionization Detector

A flame ionization detection (FID) is another analytical detector used to identify components of mixture often connected to a GC. The basic operation consists of the gaseous sample entering the column, separating, and then moving into the next portion of the device. The separated sample combines with air and hydrogen and then is combusted. The ions released from the combustion reaction are collected via a voltage potential then detected from the resulting current. Inert make-up gas is also supplied to the combustion environment to optimize the analytical conditions for detection of the elutes. In most cases, nitrogen or helium are additionally added for this purpose. The robustness, repeatability, and cost are major advantages of this detection system over similar instruments. Also, the wide linear operation range of the detector on the order of

10^7 is another reason this detector is used often with gas chromatographs. The FID is considered the best detector for hydrocarbons, but tends to have lower intensities when oxygenated molecules are involved due to lower ion formation from the combustion stoichiometry. A disadvantage of the detection system is that CO and CO_2 cannot be detected so other means must be implemented, such as a micro-GC, for these gases. The theory behind the detection system is based on the ion production from the resulting hydrogen flame. The current detection is directly proportional to the amount of carbon in the molecule on the basis of 1 ion per 106 carbon atoms [44]. The concepts of interest are the specific ions formed in the flame and chemical reactions taking place in the pre-combustion zone.

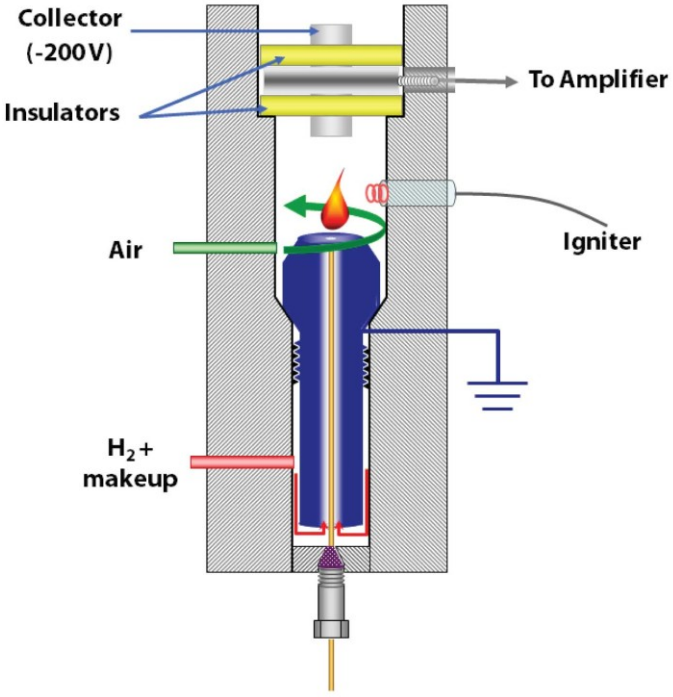

Figure 2.7: Flame ionization detector internal diagram [44]

Holm's review of the FID flame chemistry depicts a transformation as the elutes move up the chamber [45]. He suggests that compounds are stripped to unsaturated components to form methane which is then combusted later in the flame to form the important CHO^+ ion. This theory supports why the detection is directly linked to the amount of carbon atoms in a sample.

2.6.4 Coupled Studies and Main Products Fast Pyrolysis

If identification is to be implemented in a fast pyrolysis experiment, the most common method is performed by directing the gas products directly into a chromatography column linked to a mass spectrometer, often denoted Py/GC/MS. This method is fairly simple to execute since small sample sizes are applicable and many instruments are designed to be coupled together.

Characterization of the product distribution from cellulose, hemicellulose, and lignin has been carried out by Patwardhan et al. in a furnace micro-pyrolyzer at 500° C attached to a GC/MS [38, 46, 47]. Cellulose contained largest yield of any one component, with levoglucosan accounting for 58.8 wt% of the product distribution. A similar analysis was performed for hemicellulose with the most abundant compound being formic acid. For lignin, 24 major compounds were identified, and 93% of total mass balance was accounted for with the largest volatile component fraction being acetic acid. For these experimental results a flame ionization detector (FID) was used for quantification calibration for each compound, but identification was done with a mass spectrometer.

Wu et al. pyrolyzed a model compound of cellulose, glyceraldehyde, and analyzed it with a GC/MS; Figure 2.8 displays the results in form of a chromatogram. Each peak represents a different compound elucidating from the column at different retention times. Attaining the product distribution with quantitative analysis allows for more detailed pyrolysis models to be formulated about the fundamental reactions. There are limitations to this technique as contamination of the column could alter results, and quantification is a time consuming process to calibrate from pure standards. Also, secondary reactions could occur in the column resulting in poor interpretation of the data collected *in situ* within the reaction zone. For these reasons, and because of the lack of time resolution, it is of interest to find a method based on non-intrusive optical sampling.

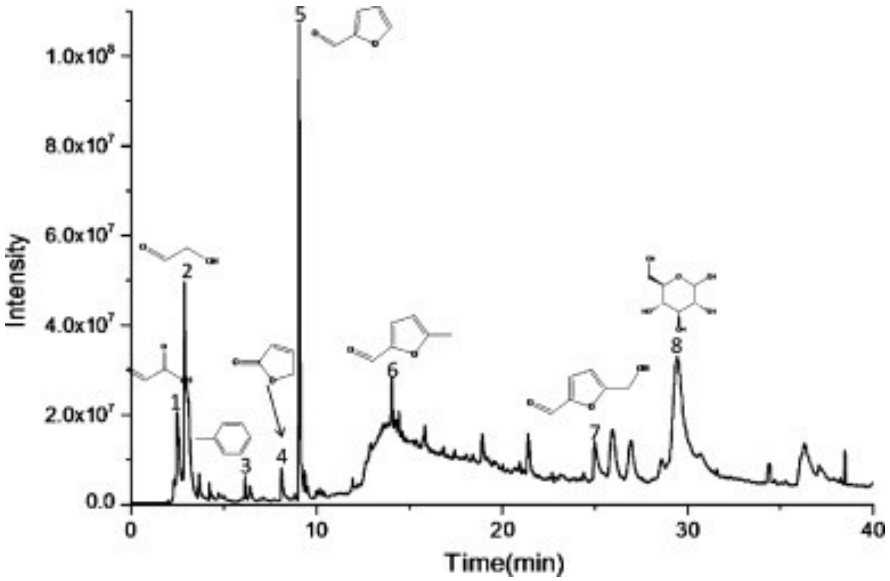

Figure 2.8: GC/MS spectrum of the pyrolysis products of glyceraldehyde [48].

CHAPTER 3. EXPERIMENTAL SET-UP

3.1 Bench Scale Pyrolysis Flow Cell

A bench scale pyrolysis flow cell, as shown in Figure 3.1, was designed and fabricated to enable testing of the proposed optical diagnostics. The goal was to provide a means to establish conditions that mimicked the pyrolysis process. The design parameters were:

- Optical access on at least two sides with removable windows
- Ability to reach temperature of 500° C
- Ability to insert biomass *in-situ*
- Purge oxygen out of the cell

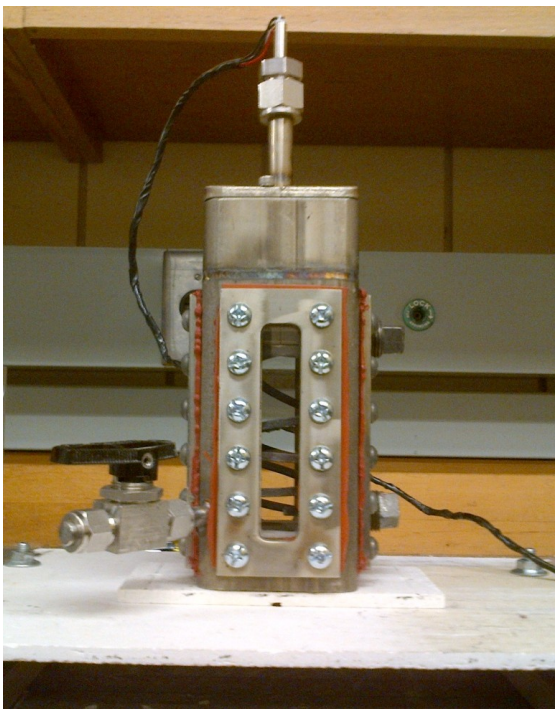

Figure 3.1: Pyrolysis flow cell with optical access.

- Mobility to move cell to different locations to perform various diagnostic techniques

The material of the outer shell consists of 304 stainless steel rectangular tubing with recessed window openings with dimensions of 1" by 4.25". Also, on each side 12 tapped screws were machined to hold the windows in place with stainless steel outer plates. High temperature resistant silicon gasket material placed in between the cell window and outer plate to help with sealing the cell. A removable lid was used to support the internal coil heater and contain am exhaust port for the escaping gas and volatiles. Ceramic insulation was used to insulate the interior of the cell to provide an isothermal environment. Biomass was inserted through a welded port near the bottom attached to a 3/8" Swagelock ball valve.

The heating system consisted of two units, which were implemented to get the cell up to the desired temperature. A 500 W Omega inline heater was used to heat the nitrogen gas supply in conjunction with a coil heater to keep the cell at constant temperature. The heater was an Entherm 690 Watt 965 mm straight resistance wire with 2.2 × 4.2 mm cross section which supplied heat within the cell. The heater was coiled into a helical shape on site to fit inside within the walls of the cell. A resistance coil was chosen to maintain isothermal conditions in the cell due to the ability to be bent to shape and allow open spaces to apply laser transmission through the cell at various locations downstream of the pyrolysis zone. The coil heater was powered by a 120-230 V step up transformer, which in turn was connected to a proportional temperature controller. Three type K thermocouples were placed within the cell at three vertical locations, with

the middle thermocouple attached to the temperature controller for monitoring the process temperature.

The heating process began with flowing 25 slpm of nitrogen through the cell with the use of an Aalborg rotameter. The inline heater and temperature controller were switched on to begin the heating, and the cell was allowed to reach steady state conditions. After the bottom and middle thermocouples were reading within 30° C of each other, testing could commence by inserting samples one at a time. Liquid samples were inserted using a 2.5 cc syringe with a 6 inch, 20 gauge stainless steel needle. Solid samples were weighed using a laboratory balance and placed into a small cylindrical sample boat and inserted with the device described below.

3.2 Sample Insertion

Finding a method to insert the biomass constituent samples into the flow cell was critical to prevent pyrolysis from occurring before entering the cell without affecting the flow conditions. The sample was inserted into the chamber by using a piston push method from pressurized nitrogen. A ¼ inch nylon tubing line from the regulator to a ball valve with nitrogen was pressurized to 15 psi to create potential energy for pushing the piston. The valve was quickly turned to allow the gas expansion to push the sample into the reactor by a small cylindrical piston. A stainless steel sample boat was pushed into the hot cell and the sample was exposed to the high-temperature environment. Although a method for establishing a static sample was desired, the current proof-of-concept demonstrations were conducted with the sample being entrained into the hot nitrogen flow. This method allowed for quick insertion into the hot environment of the

cell without disturbing the reaction volume. Figure 3.2 shows cellulose being entrained in the nitrogen flow after insertion, as applied for all experimentation with FTIR.

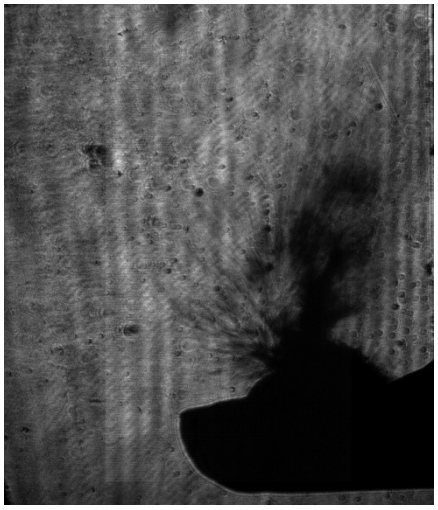

Figure 3.2: Schlieren image of 10 mg of cellulose inserted into the pyrolysis cell.

Another system employed for sample insertion was a gravity fed batch feeder system to allow for continuous operation. This system relied on gravity and a small motor to agitate the sample and fall down a 1/8 inch stainless steel tube which protruded to the bottom of the cell. The hot nitrogen flowed around the smaller insertion tube into the reactor through a 3/8 inch stainless steel tubing. The sample was loaded from the top agitated and entrained into the reaction zone with the gaseous products to be analyzed by the GC/FID detection system. A batch system was needed in order to fill the gas sampling loop with elutes that could be injected into the column via the gas sampling valve. Figure 3.3 shows the batch feeder system with the agitation motor and inline heater connected on the side.

Figure 3.3: Batch Feeding system for GC/FID experimentation

3.3 Temperature Characterization

A national instruments cDAQ-9172 was used in conjunction with LabVIEW Signal Express software to monitor three Omega type K thermocouples at different vertical locations within the cell. The temperature probes were placed in the center of the cell to attain the centerline temperature within the coil to track the temperature at the measurement location. The center thermocouple was also connected in parallel to an Omron E5C2-R40K controller to maintain a constant temperature. A built in cold junction source from the data acquisition system was used for compensation to attain the absolute temperature from each thermocouple. The data was plotted at sample rate of 1 Hz with the temperature and time stored on the hard disk to be processed.

3.4 FTIR Experimental Configuration

To inspect the infrared absorption spectra and study the chemistry of cellulose and lignin pyrolysis, the cell was used with a modified FTIR spectrometer, as shown in Fig. 3.4. A Varian 680 FTIR system was used for all testing with an installed internally

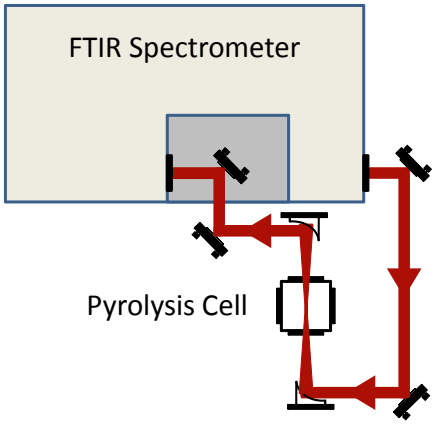

Figure 3.4 Optical setup of pyrolysis Cell with FTIR

controlled pop up plane mirror installed. The mirror diverted the infrared beam outside of the instrument and to the reactor rather than to the sample compartment. The system was enclosed with 4 inch pvc pipe as beam tubes and Lexan plexiglass to encase the cell. The encasement was purged with dry air to prevent water vapor and carbon dioxide from entering the beam path between background and sample runs. To direct the beam to the pyrolysis cell, 4 IR reflective gold mirrors were installed. To focus the IR beam into the cell and obtain greater spatial resolution, 2 silver-plated parabolic mirrors with 6 inch focal lengths were placed on each side of the cell. The first mirror focused the beam into the cell while the second mirror re-collimated the beam to the detector. Zinc selenide windows were installed for IR experimentation for its transmission and temperature resistant properties. Removable stainless steel plates held the windows in

place and allowed the heights of windows to be adjustable. A liquid nitrogen cooled mercury cadmium telluride (MCT) detector exhibiting high sensitivity and quick response time was used for detection. These attributes allowed for the residence times of pyrolysis to be collected with time resolution and with a high signal-to-noise ratio. The collections were taken at a spectral resolution of 16 cm^{-1} with a sampling rate of 0.03 s/scan. The temperature was also monitored using National Instruments signal express software during each run. Figure 3.5 displays the entire experimental set-up of FTIR experimentation, including the purge encasement, sample injection, and temperature data acquisition equipment.

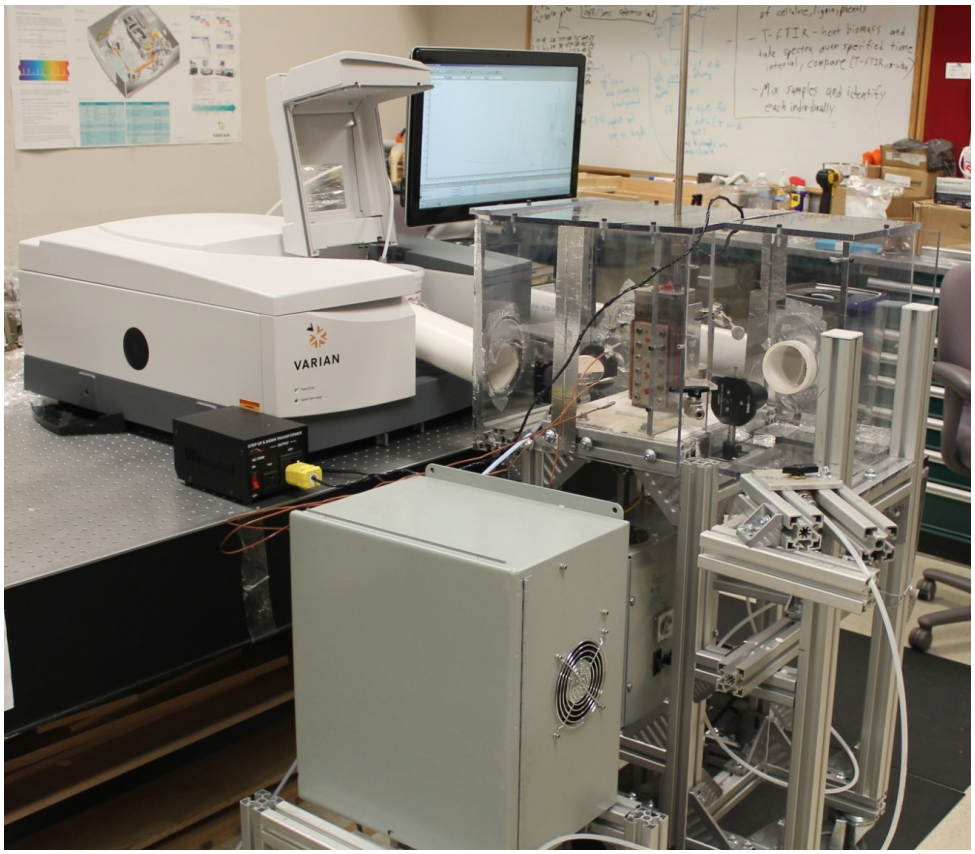

Figure 3.5: Experimental apparatus of the FTIR set-up.

3.5 GC/FID Setup

A Bruker 436 Gas Chromatograph ® (GC) with a flame ionization detector was used for experimentation to identify the main gaseous components of the pyrolyzer and ensure the new instrument was running to the standards of other bench scale micropyrolyzer systems. A phenomenox ZB-1701 column (60 m x 0.250 mm and 0.250 μm film thickness with stationary phase consisting of 14% cyanopropylphenyl and 86% dimethylpolysiloxane phase) was used for all experimentation. The oven program consisted of 3 minutes at 35°C, ramping to 300°C at a rate of 5°/min, and holding this temperature for 4 minutes for a total run time of 60 minutes. Compounds were calibrated using 1 μL manual injections with 1:100 split ratio at a injector temperature of 280° C. Helium was used as the carrier gas through the column and was kept at a constant flow rate of 1 ml/min. The FID was set to a temperature of 300° C with the flow conditions of 25 ml/min helium make-up gas, 30 ml/min hydrogen, and 300 ml/min of air. Eighteen compounds were calibrated to attain elution times for each component so identification could be made during pyrolysis experimentation. Figure 3.6 displays the typical chromatogram of cellulose pyrolysis with GC/FID instrumentation. Figure 3.7 shows the cell in an inverted position for experimentation with the GC/FID.

The gases from cellulose and lignin pyrolysis were analyzed with the use of a 6 port Valco gas sampling valve directly plumbed onto a 250 μL sample loop. The cell was inverted to allow for the gravity feeder to be implemented with the exhaust port plumbed directly into the sampling valve. The fittings from the cell to the inlet of the GC/FID were wrapped with heat tape to maintain temperatures near 300°C to prevent

condensation of gaseous components. A 7 μm Swagelok filter was attached inline to prevent particulate matter from entering the plumbing to the valve system.

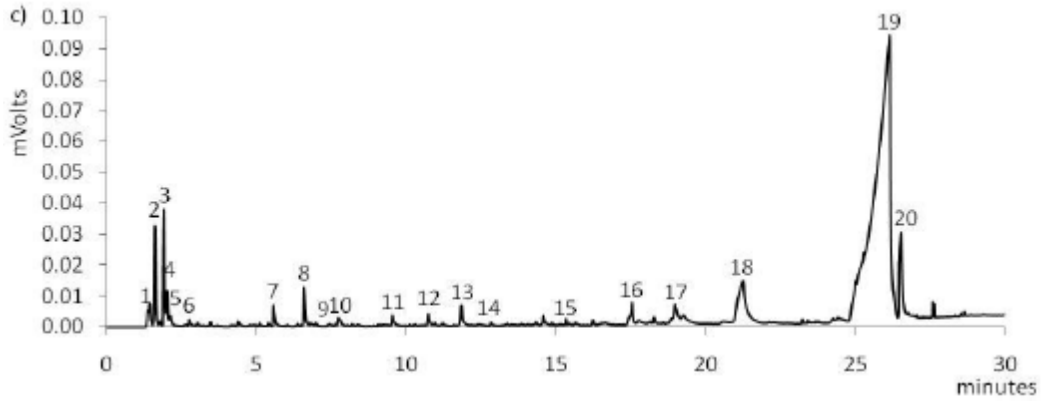

Figure 3.6: GC/FID chromatogram of cellulose [49].

Figure 3.7: Inverted cell for GC/FID gas analysis.

The experiment started by heating up the cell to 500°C and applying 10 V to the agitation motor to feed the particles into the reactor. After 2 seconds the temperature program was initiated and a pneumatic sampling valve was switched to injection mode with the Compass software program. The sample loop was then injected onto the column and analyzed to obtain a voltage versus time chromatograph.

3.6 Coherent Anti-Stokes Raman Scattering Experimentation

A vibrational hybrid fs/ps CARS setup was used to observe Raman active transitions in phenolic compounds within the cell. A Spectra-Physics Solstice femtosecond pulsed laser, a Spectra-Physics TOPAS optical parametric amplifier, and a home-built 4*f*-pulse shaper were used to attain the pump, Stokes, and probe pulses at the desired wavelengths and pulse shapes. Figure 3.8 shows the experimental configuration of the optics and the location of the heated cell with relation to the pump, Stokes, and

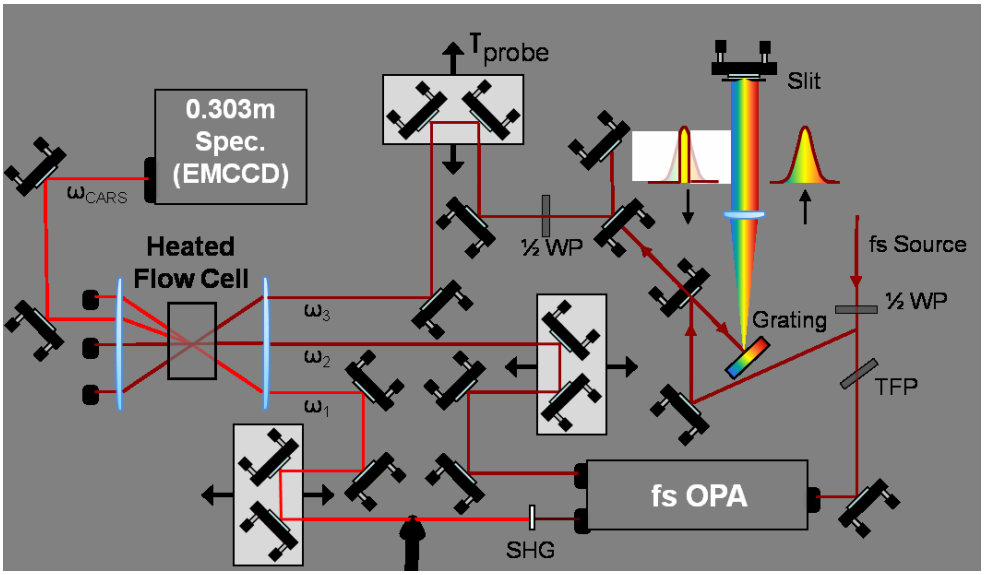

Figure 3.8: CARS configuration used for probing phenolic compounds within heated cell.

probe beams. The CARS signal was collected and measured with a 0.303-m (Shamrock SR-303i, Andor) spectrometer. The 0.303-m spectrometer uses a 1200 line/mm grating achieving an instrument resolution of 2.4 cm^{-1} with an electron-multiplied charge coupled device (EMCCD) Newton camera. The frequency of the pump pulse was altered to access the transitions of interest, whereas the Stokes and probe remained constant at 795 nm, the fundamental output of the Solstice. Figure 3.9 shows the

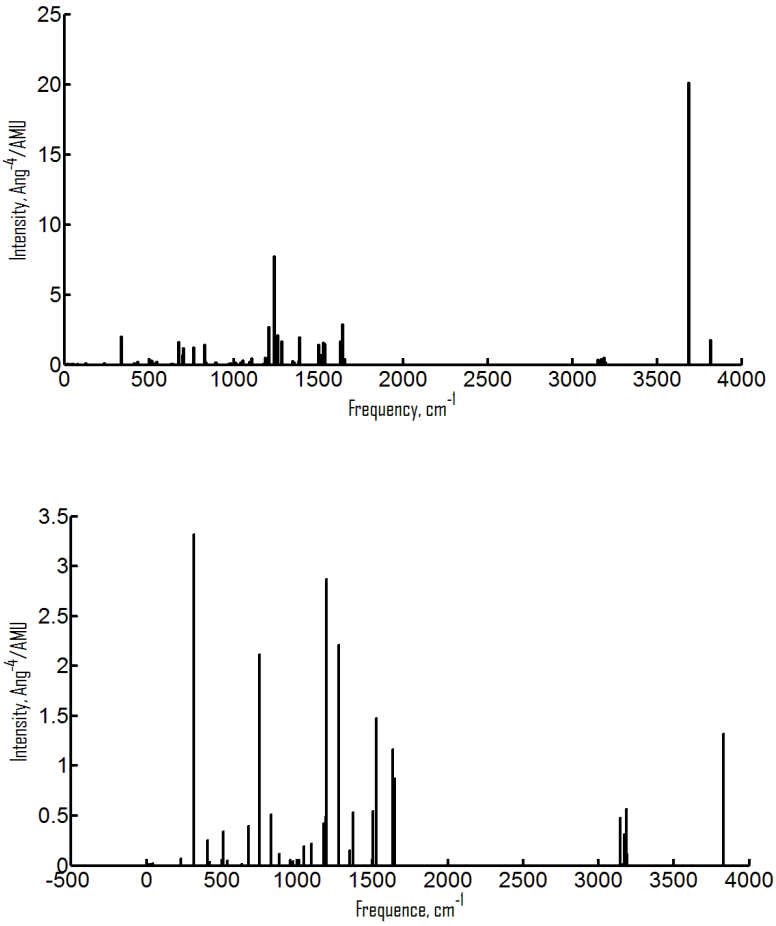

(a)

(b)

Figure 3.9: Spectral model of phenol (a) monomer and (b) dimer frequencies.

modeled frequencies of a phenol monomer and dimer [Ganesh Balasubramanian, personal communication, 2013], which provided insight into transitions probed during the experiment.

The pump was chosen as 619 nm to access a Raman transition around 3550 cm^{-1}. It is believed that this corresponds to the OH-stretch of phenol, which should occur around 3373 cm^{-1} for the phenol monomer based on the literature [50]. The actual wavelength might be skewed due to the spectrometer not being calibrated absolutely, as well as due to beam steering into the spectrometer. The timing of the probe pulse was altered during experimentation once signal was obtained. This was accomplished with a motorized delay stage (ILS150PP, Newport) with a resolution of 5 μm. The probe pulse timing was altered to suppress non-resonant signal and view the changes in the spectrum over a specified time period to learn more about the properties of phenolic molecular response in time. This is the first time- and frequency-resolved CARS data recorded for phenols to the author's knowledge.

Heated window extensions were added to the main cell body to prevent the glass from being damaged and allow enough room for the beams to cross near the center of the cell, as shown in Figure 3.10. The window extensions were heated to prevent condensation of the gasified compounds on the interior window surfaces. Samples were inserted into the cell via a cylindrical stainless steel rod with a notch cut out to hold the compound. The cell was heated above the boiling point of the sample and the sample was vaporized. This vapor was then probed with the goal of obtaining CARS signal to

test the ability to yielded information on time and frequency domain characteristics to differentiate between phenol and biphenol.

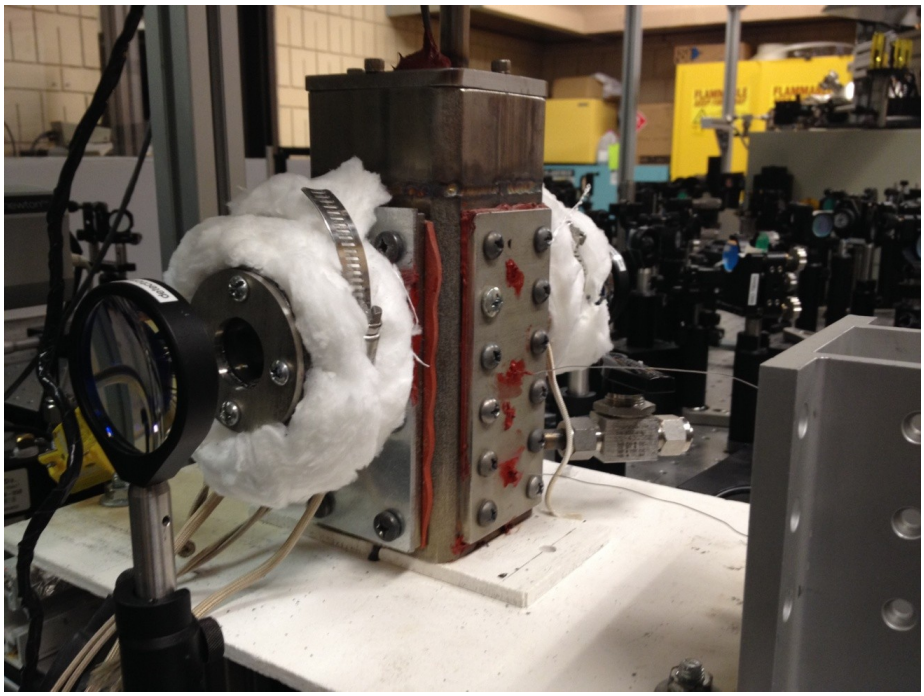

Figure 3.10: Heated cell with window extensions in CARS setup.

CHAPTER 4. RESULTS AND DISCUSSION

4.1 Temperature Profile Results

The process temperature was recorded at three distinct locations of 31, 76, and 116 mm from the bottom of the cell. A heated nitrogen flow rate of 25 slpm was used to heat the cell along with the coil heater. Figure 4.1 displays a plot of the heating process within the cell to 500° C reaching steady state conditions. The cell takes nearly 10

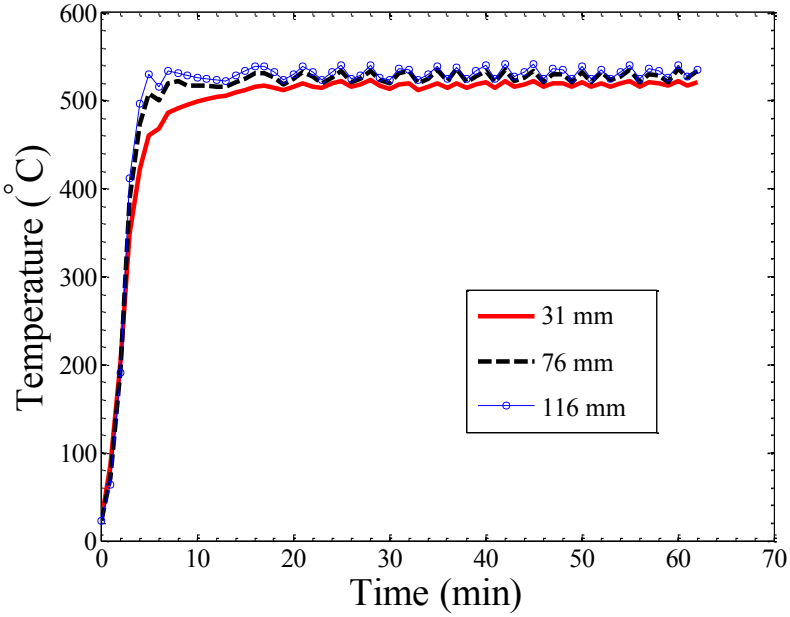

Figure 4.1: Temperature vertical profile of pyrolysis cell with an accuracy of ±6° C.

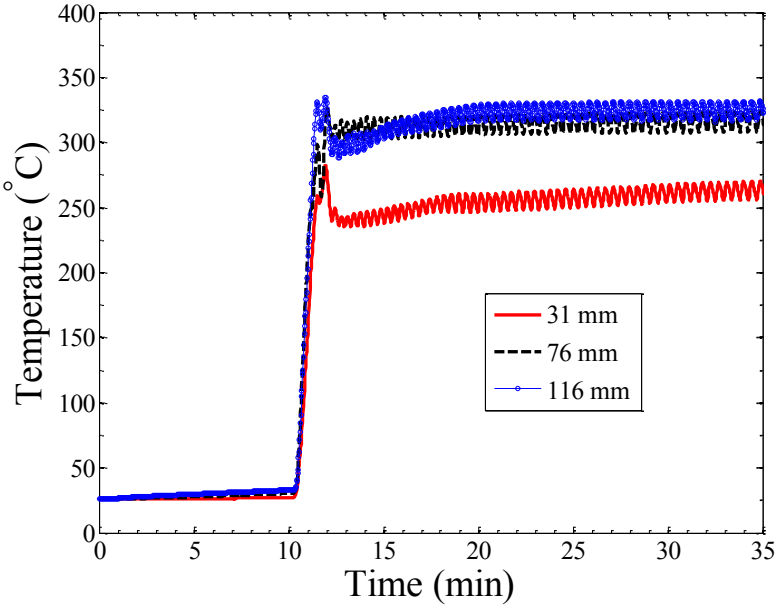

Figure 4.2: Temperature profile of cell with heated windows.

minutes to reach isothermal conditions, with temperature differences between the top and the bottom being about 30° C. The difference in temperature is attributed to non-uniform heating from the coil heater and some heat loss through the sides of the reactor. The resistance wire was coiled into 8 coils uniformly distributed for all tests flowing through the cell.

Another temperature profile taken at the same locations and shown in Figure 4.2 was collected when there is no heated nitrogen flow to characterize the conditions used for CARS experimentation. All heating was done by the coil heater stretched so there is space for the beams pass through without being block and to place the sample holder. To minimize temperature stratification the coils were densely placed near the sample at the bottom of the cell. Figure 4.2 shows the temperature plotted over time when steady state conditions are met with an initial 10 minutes of heating of window extensions on the cell for CARS experimentation. The difference between the top and bottom temperatures was about 40° C for this condition. To ensure vaporization of the samples, the controller was always set above this temperature difference.

4.2 FTIR Results

Four samples consisting of cellulose, xylan, lignin, and red oak were pelletized in KBr powder and analyzed using transmission infrared spectroscopy within the sample compartment of the FTIR spectrometer. This provided a standard and a starting point for

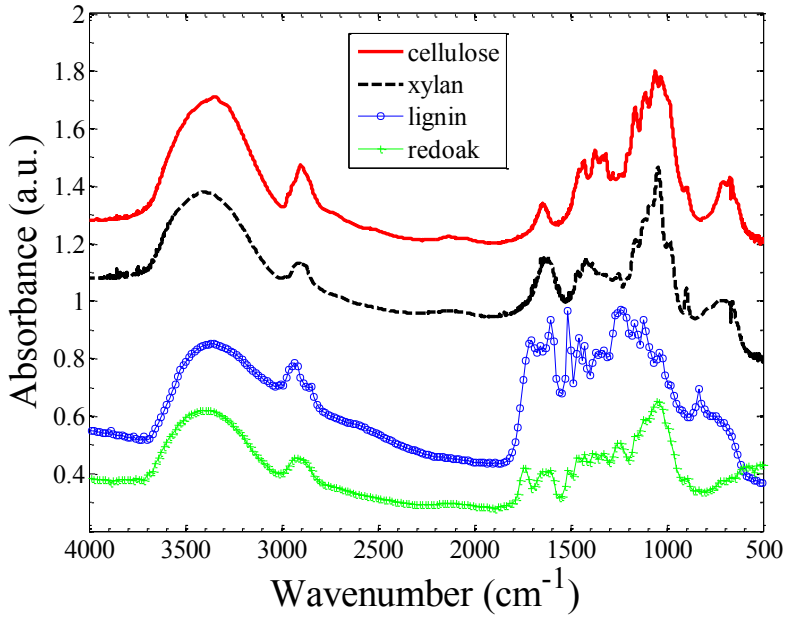

Figure 4.3 Spectra of pelletized fundamental biomass components.

observing the main spectral features before pyrolyzing cellulose and lignin in the cell. The spectra, as shown in Figure 4.3, were attained with a resolution of 1 cm^{-1} and averaged over 16 scans with a background subtraction applied to all the spectra. Each sample contains a distinctive wide peak centered at 3400 cm^{-1} and 2900 cm^{-1} corresponding the OH and CH stretches respectively. There are broad peaks in cellulose, xylan and red oak near 1050 cm^{-1} corresponding to C-O stretching and deformation. The fingerprint region from 1800-700 cm^{-1} displays distinct differences between the biomass constituents. Red oak and lignin show many more features in this region due to aromatics being more prevalent in these compounds leading to many bands of C=C stretching and methoxyl-O-CH_3 functional groups. Red oak contains all three components and that is shown in the spectra containing functional groups of each constituent component.

Cellulose and Lignin were inserted into the cell and fluidized in the hot flow in a 500° C environment. In Figure 4.4, a profile of cellulose is plotted with respect to different residence times in the cell. Assuming laminar flow through the cell the linear velocity of heated nitrogen flow was 21 cm/s. The residence times could then be calculated based on the distance from the insertion to the IR-probe location. At the residence time near the insertion point (70 ms) there are few structures identified, but as the time increases many functional groups can be labeled.

The most prominent broad absorbance peaks occur at 3530 cm^{-1}, 2350 cm^{-1}, 2905 cm^{-1}, 1725 cm^{-1}, and 1069 cm^{-1}. The first two are due to OH and CH asymmetric stretch as previous seen in the pelletized samples. The asymmetric stretch of CO_2 is

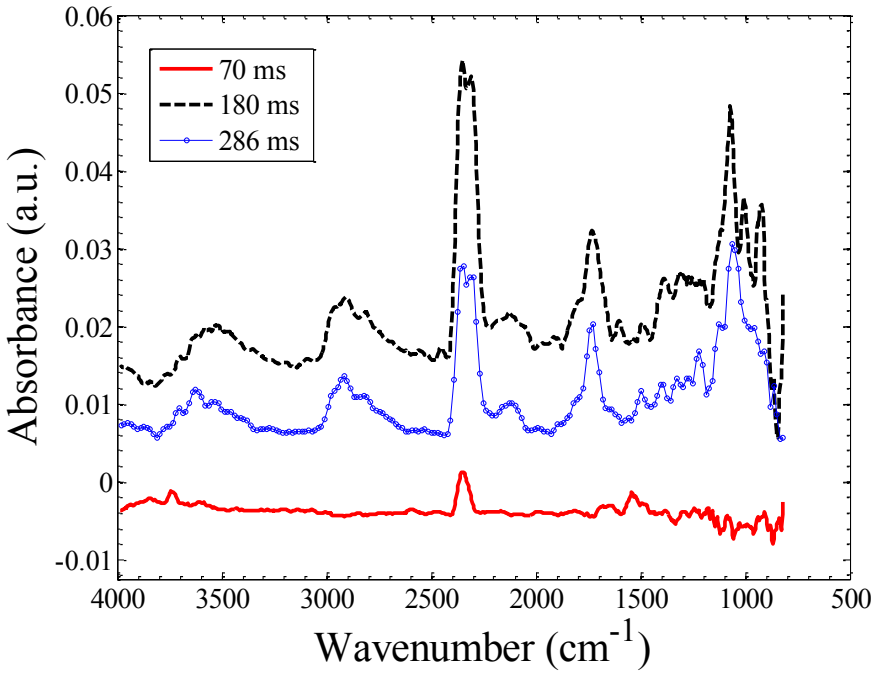

Figure 4.4: A cellulose spectral profile at different vertical heights within the pyrolysis cell corresponding to varying residence times.

most prominent and the peaks rise with residences times at 2350 cm^{-1}. The latter two absorbance peaks can be attributed to C=O double bond stretching and C-C, C-O stretching. Based on literature these compounds in formation could be found in classes such as alkanes, aldehydes, ketones, carboxylic acids, and alcohols [51]. Two significant peaks arise at 180 ms at 1002 cm^{-1} and 926 cm^{-1} which don't appear at 286 ms and which could be C-C skeletal vibrations exposed during the initial cleavage during pyrolysis that get reformed at a later point in time. Again the same main features of OH, CH and CO_2 are observed when pyrolyzed with absorbance bands not being prevalent until 180 ms. Between 180 and 286 ms the main regions where differences arise is 1800-1500 cm^{-1} and a broad region near 1200 cm^{-1}. The ratio and shape of the structures near 1600 cm^{-1} is due to splitting and reformation of aromatic ring structures which are highly dependent on the position and nature of the elements on the ring itself.

The results for lignin pyrolysis are similar, as shown in Figure 4.5. The broad peak centered around 1200 cm^{-1} is consistent with a the phenolic C-O stretch of phenolic compounds which could be due to splitting and reforming near 286 ms.

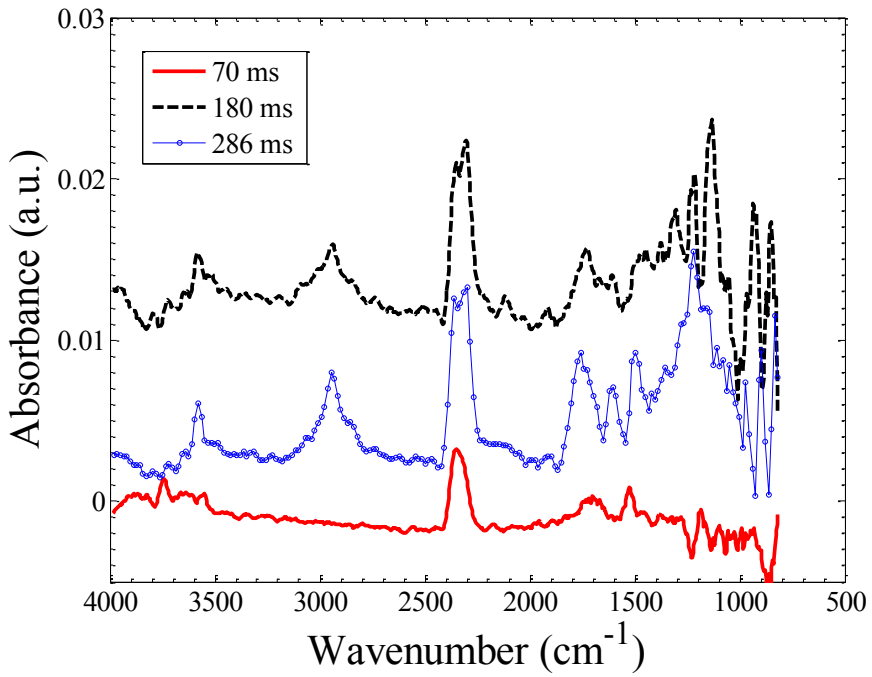

Figure 4.5: A vertical spectral profile of lignin at varying residence times.

Phenolic model compounds were also vaporized and observed with the FTIR through the flow cell. The spectra in Figure 4.6 demonstrate how even very similar compounds can contain different spectral signatures especially in the region from 2000-1000 cm^{-1}. The strong bands common in all three spectra are OH stretch, OH bend, CH stretch, and C-O, at 3600 cm^{-1}, 1350 cm^{-1} , 3000 cm^{-1}, and 1200 cm^{-1}, respectively. For guaiacol, there are peaks observed at 2950 cm^{-1} and 2850 cm^{-1} that correspond to the CH stretch in the methoxy group (CH_3-O-). Aromatic ring stretching is typically centered around 1600 and 1500 cm^{-1}, which is readily present in phenol and guaiacol. Since the concentration is lower in the 4-vinylphenol solution, those peaks are not as pronounced. The entire molecule has an effect on spectra and the locations of the peaks, so most

functional groups do reside within a range in which they can overlap. However, by analyzing the features in further detail, a good idea of what is being probed in the sample of interest can potentially be gained.

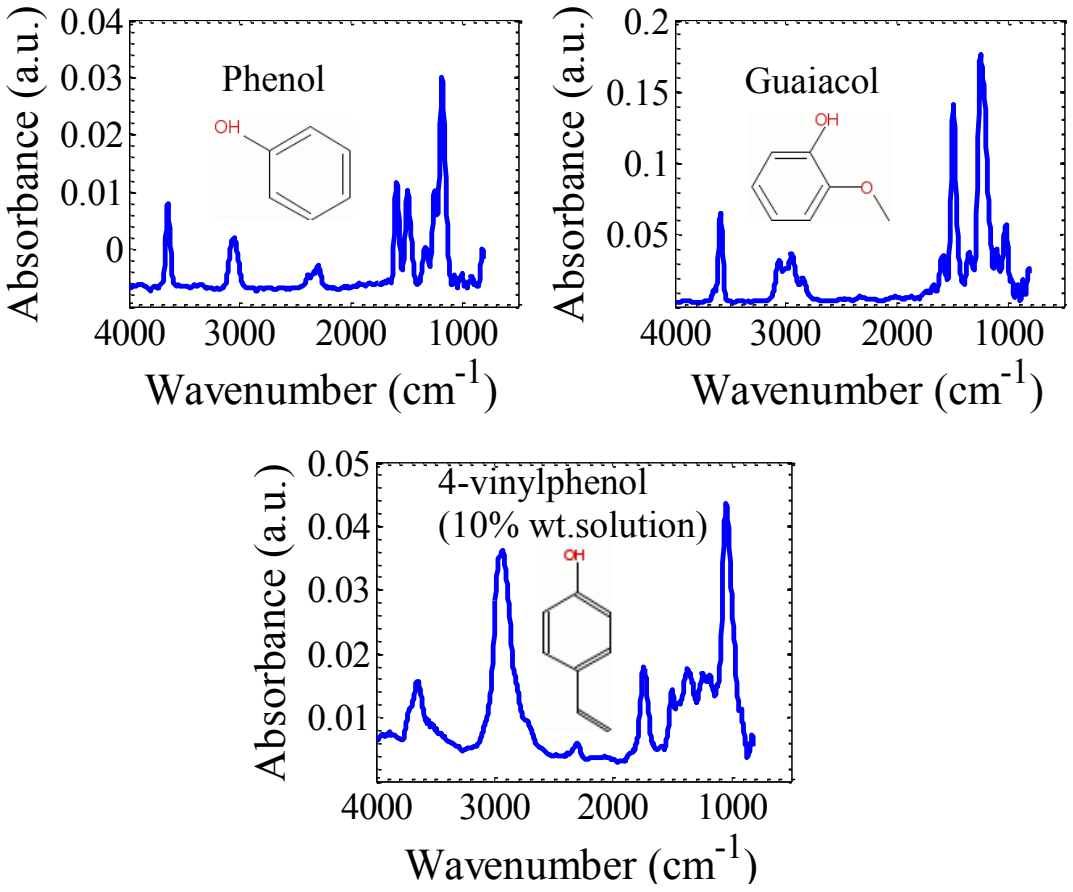

Figure 4.6 Vapor spectra of phenol, guaiacol, and 10% 4-vinylphenol in propylene glycol.

4.3 CARS Results

The CARS data represent Raman spectra and as such are complementary to the FTIR results. They also hold the potential to provide spatio-temporal resolution with the sample chamber, since the laser beams can be focused to within 10's of microns of the a sample of interest. The current results represent proof-of-concept demonstrations only since the CARS spectra for pyrolysis products are not readily available in the literature. Moreover, the data presented here encompasses both frequency (spectral) and time-domain measurements since the excitation and probe pulses are fs and ps pulses. The frequency domain plotted in a similar fashion as the FTIR spectra. However, the time domain represents the data obtained as the probe pulses is delayed over a period of 10's of ps after the excitation pulses, and this time delay can potentially provide additional information.

Time-domain measurements were obtained by altering the delay of the probe pulse and observing the frequency response over a 100 ps time frame. The probe pulse was spectrally narrowed using a home built 4*f*-pulse shaper consisting of a grating to disperse the light, a cylindrical lens for collimation, and an adjustable slit in front of a mirror to serve as a mask. The probe pulse passes through rectangular slit in the frequency domain, yielding a sinc^2 time profile. The slit width was chosen to provide a probe pulse with a bandwidth of approximately 4.5 cm^{-1}. In Figure 4.7 the probe pulse and best-fit sinc^2 profile are shown as a function of time.

In order to suppress nonresonant signal, probe delays corresponding to a nonresonant background decrease of at least two orders of magnitude were chosen.

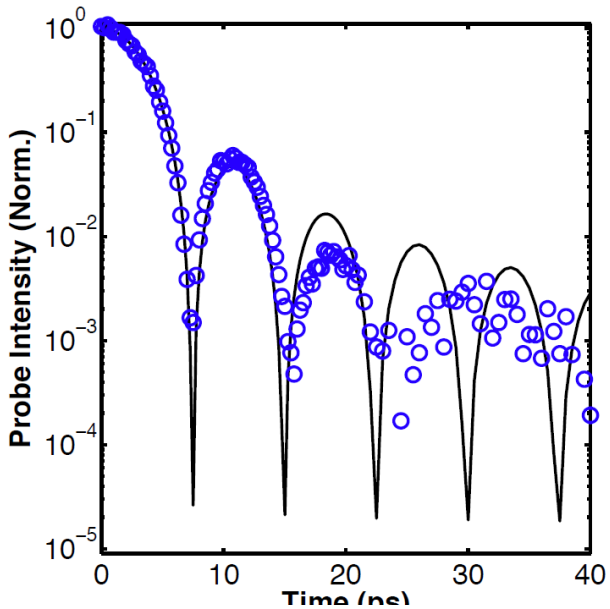

Figure 4.7: Experimental and theoretical time profile of the probe pulse.

Specifically, the first two probe delays corresponding to minimum nonresonant signal, 7.5 ps and 15.75 ps, are of interest. Additionally, time delays greater than 22 ps show the nonresonant signal to be below the noise threshold of the data, and shall also be considered.

The subsequent plots will show the data collected at these different probe delays. A spectrogram (plot of spectrum vs. time) of phenol and 2,2'-biphenol are shown in Figure 4.8, with the color distribution representing the signal intensity at a given point in time and frequency. The overall shapes of each scan are similar, but when looking at a spectrum at one particular time delay there are distinct differences. For example, at the times of minimum non-resonant background (to allow the cleanest data to be collected) at 7.5 ps and 15.75 ps, there are clear differences in the shapes of the frequency response. At a later time delay of 33.5 ps, the overall spectral features are similar, but

intensity ratios between similar features are different between phenol and 2,2'-biphenol. This is promising as a means of distinguishing monomers versus polymers of various compounds. Phenol and 2,2'-biphenol spectra overlap in frequency; both compounds exhibit spectral responses in the range of 3500-3575 cm^{-1}. However, by choosing an optimal probe delay, it is possible to elucidate which compound is present with high temporal and spatial resolution. In order to further this work and gain specific concentration measurements from spectrally overlapping phenolic species, a model is needed to correlate the time domain response with actual concentrations of a given species. Although not undertaken here, the CARS technique could also be useful for measuring temperature *in-situ* within reactors during fast pyrolysis processes to gain valuable information regarding heat transfer and reaction kinetics. The ability to measure temperature, in fact, has been the main application of this technique in past studies, and it is possible to measure with 10's of microns from a reacting surface. In the current work, the main interest was in demonstrating the feasibility for also identifying certain species that would indicate the formation of undesirable heavy compounds. This proof-of-concept demonstration will need to be expanded to include heavier compounds, but this was a successful demonstration of the ability to provide optical access for such measurements during pyrolysis reactions. As such, it is of interest to survey other molecules that are relevant for evaluating the product evolution for various pyrolysis conditions and in the reacting boundary layer.

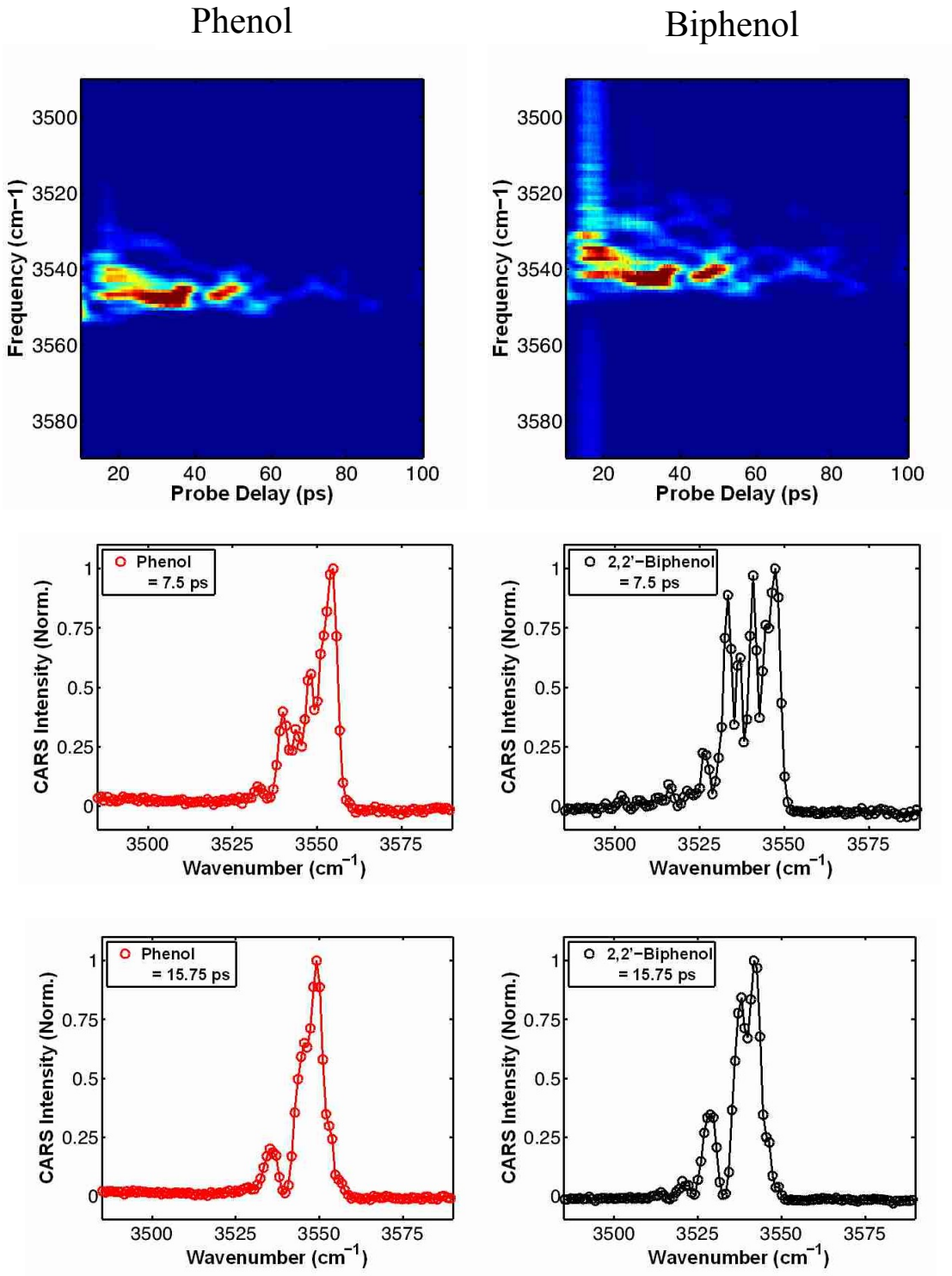

Figure 4.8: Time domain of phenol and bipheonol with cross sections taken at minimum non-resonant times of 7.5 and 15.75 ps.

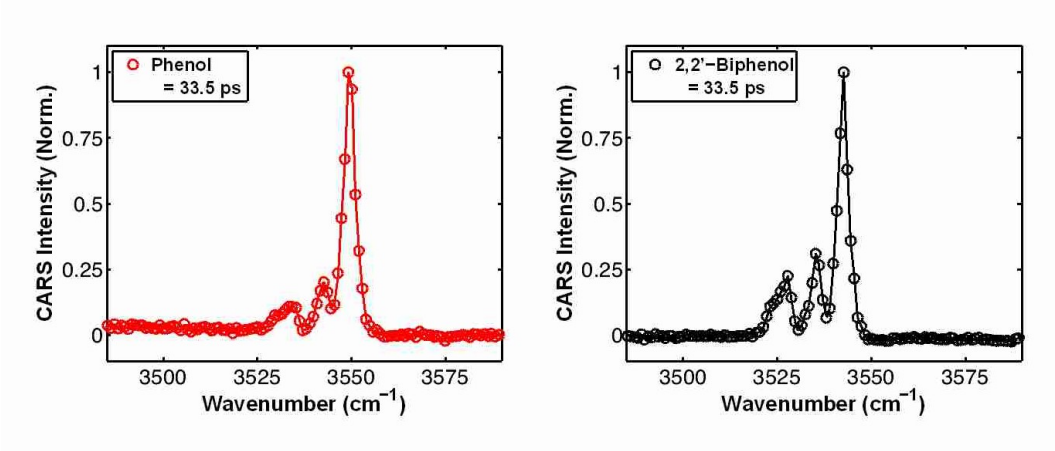

Figure 4.9: Profile of phenol and biphenol at 33.5 ps time delay

4.4 GC-FID Results

Although not performed *in situ*, the Bruker GC/FID measurements were used to separate gaseous components and confirm that appropriate products were being released from cellulose and lignin pyrolysis. Eighteen compounds were calibrated to attain the elution time through the column with the Bruker GC/FID instrument. From the elution times, the products could be identified from the reactor. Based on these elution times compounds could be identified from pyrolyzing the samples. For this analysis, a mass balance was not performed since that would require producing a calibration plot based on concentration and peak area. Table 3 displays all the compounds of interest based on the work of Patwardhan [49]. These compounds only represent a sample of the all the gaseous species present from fast pyrolysis of cellulose and lignin.

The lower molecular components elute first from the column shown in the region from 5-10 minutes with large molecules eluting later in time. A major peak is shown at 42.5 minutes, signifying levoglucosan is present which is a major component of

Table 4.1: Elution times of calibrated compounds in GC/FID.			
Peak Number	**Compound**	**Elution Time (min)**	**Solvent**
1	Acetalhyde	5.41	Acetone
2	Furan	6.09	Acetone
3	2-methylfuran	7.73	Acetone
4	Glycolaldehyde	~10	Methanol
5	Acetic acid	11.2	Methanol
6	Hydroxyacetone	12.51	Methanol
7	Furfural	18.21	Acetone
8	Fufural alcohol	19.54	Methanol
9	5-methylfurfural	22.74	Acetone
10	Phenol	25.80	Methanol
11	2-methoxyphenol (Guaiacol)	26.52	Methanol
12	4-vinylphenol	33.0	Methanol
13	2-methoxy-4-vinylphenol	33.19	Methanol
14	5-(hydroxymethyl) furfural	34.17	Acetone
15	2,6 dimethoxyphenol	34.56	Methanol
16	4-methyl-2,6, dimethoxyphenol	36.81	Methanol
17	3',4'-dimethoxyacetophenone	39.99	Methanol
18	Levoglucosan	42.5	Methanol

cellulose fast pyrolysis. In most studies it is found that levoglucosan yields approximately 50-60% by weight for pure cellulose [49, 52]. In Figures 4.10 and 4.11, the peaks are labeled according to the peak number in the table in the order of elution time.

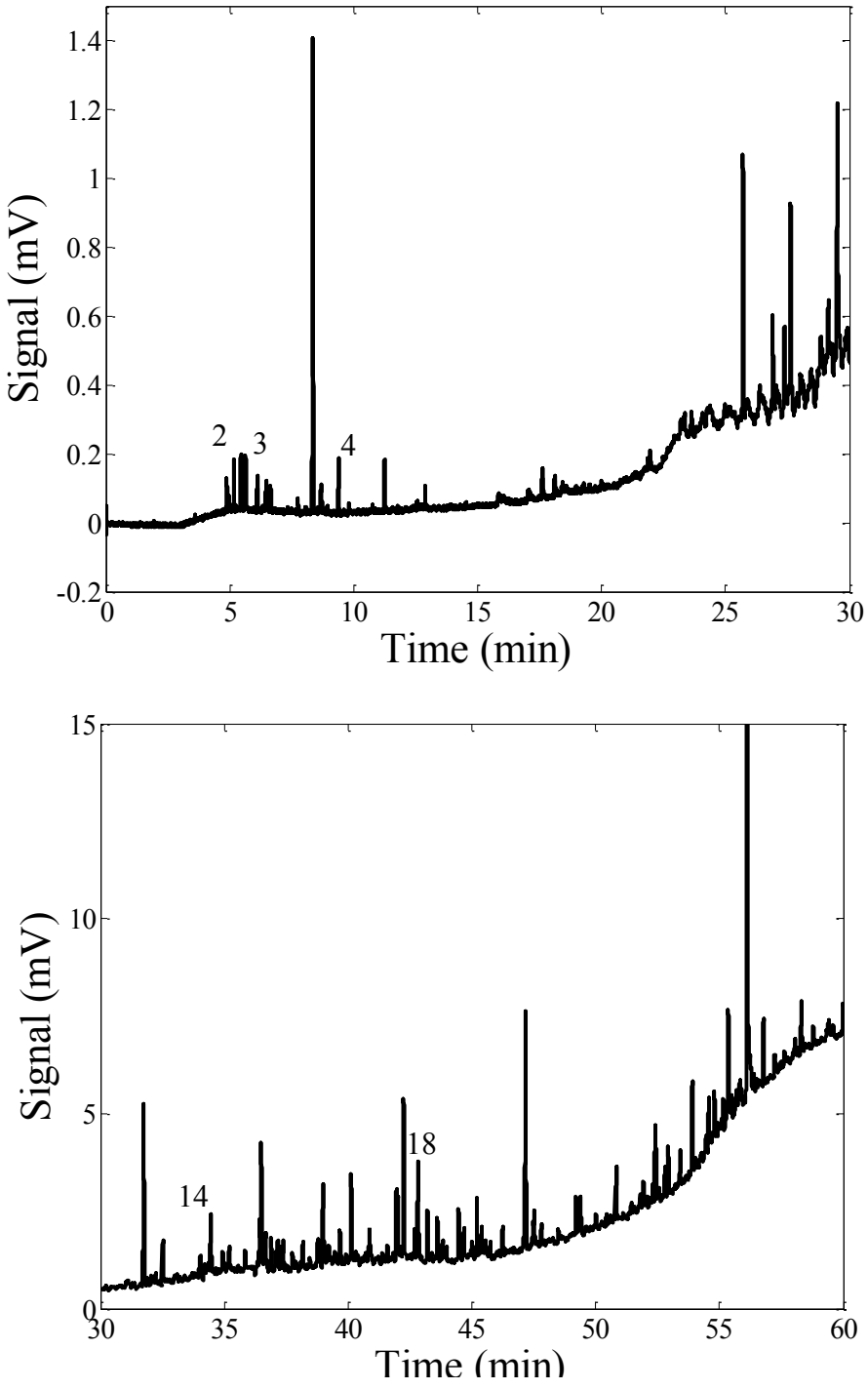

Figure 4.10: Cellulose chromatographs using GC-FID up to 60 minutes.

As for the chromotogram of lignin there seems to be missing many phenolic components that should be eluting from the column in the mid 20-30 minute range. Only 2 major compounds were identified for this chromatograph. This might be due to condensation of the elutes before entering the sampling valve or possibly the column was hampered by the impurities in the gas flow. Typically, ultra-high purity helium is used as the carrier gas, but in the case of testing the reactor standard nitrogen was used.

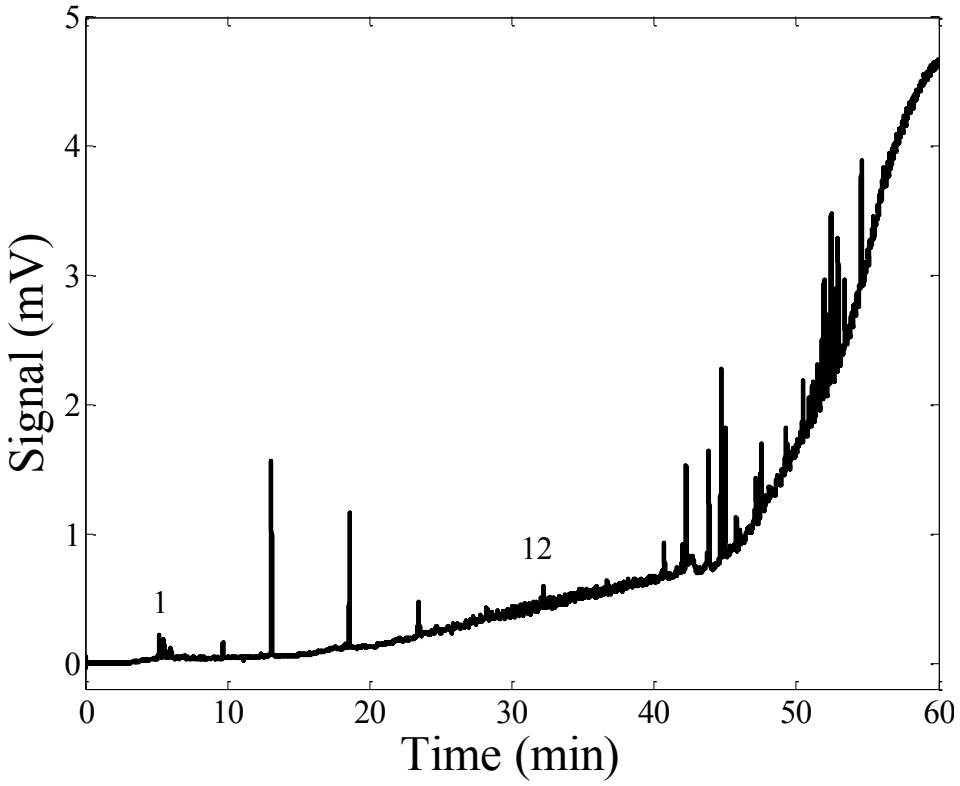

Figure 4.11: Lignin chromatograph of entire 60 minute program.

CHAPTER 5. CONCLUSIONS AND FUTURE WORK

5.1 General Conclusions

The high temperature bench scale cell reactor was developed to study the fundamental reactions in fast pyrolysis using spectroscopic techniques along with more traditional analytical experimentation. In order to accomplish the experimental goals of the work, the cell operation had to be characterized and optimized to produce conditions where relevant data could be recorded. Also, devices had to be developed to insert samples into the reactor successfully in a single action and in batch mode. The FTIR portion of the work required modifications to bring the signal beam out of a commercial instrument. This data yielded information on reaction progress and potentially on chemistry as cellulose and lignin break down during the initial stages of pyrolysis. Although, it is difficult to identify individual compounds with the FTIR, it can still be a useful tool to understand the bonding and when individual vibrations are being produced during various residence times.

Hybrid fs/ps Coherent anti-stokes Raman scattering is a new technique used for biomass pyrolysis and still needs a broader survey of species to show its relevance for product identification. However, it was shown that OH stretches from phenol and biphenol can be detected and differences are shown between the responses based on timing of the probe pulse. To the author's knowledge, this represents the first time that such time-frequency domain CARS data have been collected for products of pyrolysis. Based on this work, if monomers and polymers could be identified in the future, it may be possible to use this technique to identify product formation pathways *in-situ* during

fast pyrolysis. It can also be used for *in situ* thermometry very near the reaction zone to complement these measurements.

The GC/FID was not used in the traditional sense for fundamental chemistry research. Rather, it was used as a tool to show the multiple uses of the flow cell and identify major components of pyrolysis. Although the results identified some major products of cellulose and lignin, challenges should be addressed due to baseline instability using nitrogen in the column. There is also an issue with lignin pyrolysis that needs to be corrected for future experimentation with this technique. In the future if the GC could be coupled simultaneously to a different detection system, such as FTIR or a laser diagnostic technique, this could potentially yield useful comparisons.

5.2 Recommendations

The objective of this work was to create a functioning pyrolysis flow cell with optical access to elucidate chemistry and physics *in-situ*. Although, this is a good first step in the right direction there are a few aspects of the instruments that could be modified in the future to produce more interesting results. The reactor could be built in such a way where the flow characteristics could be known to a higher degree so that laminar flow could be validated and characterized for experimentation with residence times and physically viewing the biomass particles. For CARS work some models of the compounds of interest need to be constructed to identify and yield concentration and thermometry measurements from the pyrolysis process. The final suggestion is to develop a insertion system that is automated and can be reproduced so that human error is not involved and detailed mass balances can be obtained.

REFERENCES

1. EIA, E.I.A., *Annual Energy Outlook 2013 with Projections to 2040*. 2013.

2. Schnepf , R., *Renewable Fuel Standard (RFS): Overview and Issues* C.R. Service, Editor. 2013.

3. Scott, D.S. and J. Piskorz, *THE FLASH PYROLYSIS OF ASPEN-POPLAR WOOD.* Canadian Journal of Chemical Engineering, 1982. **60**(5): p. 666-674.

4. Brown, R.C., *Biorenewable Resources:Engineering New Products from Agriculture*. First ed. 2003, Ames, Iowa: Iowa State Press.

5. McKendry, P., *Energy production from biomass (part 1): overview of biomass.* Bioresource Technology, 2002. **83**(1): p. 37-46.

6. Rao, T.R. and A. Sharma, *Pyrolysis rates of biomass materials.* Energy, 1998. **23**(11): p. 973-978.

7. Raveendran, K., A. Ganesh, and K.C. Khilar, *Pyrolysis characteristics of biomass and biomass components.* Fuel, 1996. **75**(8): p. 987-998.

8. Yang, H.P., et al., *Characteristics of hemicellulose, cellulose and lignin pyrolysis.* Fuel, 2007. **86**(12-13): p. 1781-1788.

9. Bacovsky, D., et al., *Status of Advanced Biofuels Demonstration Facilities in 2012*. 2013, International Energy Agency.

10. *Thermochemical Processing of Biomass: Conversion into Fuels, Chemicals and Power*. 2011: John Wiley & Sons.

11. Sjostrom, E., *Wood Chemistry*. 1981, New York, New York: Academic Press, INC. 223.

12. Vanholme, R., et al., *Lignin Biosynthesis and Structure.* Plant Physiology, 2010. **153**(3): p. 895-905.

13. Broido, A. and M.A. Nelson, *CHAR YIELD ON PYROLYSIS OF CELLULOSE.* Combustion and Flame, 1975. **24**(2): p. 263-268.

14. Shafizadeh, F. and P.P.S. Chin, *THERMAL DETERIORATION OF WOOD.* Abstracts of Papers of the American Chemical Society, 1976. **172**(SEP3): p. 37-37.

15. Patwardhan, P.R., et al., *Distinguishing primary and secondary reactions of cellulose pyrolysis.* Bioresource Technology, 2011. **102**(8): p. 5265-5269.

16. Teixeira, A.R., et al., *Aerosol generation by reactive boiling ejection of molten cellulose.* Energy & Environmental Science, 2011. **4**(10): p. 4306-4321.

17. Dauenhauer, P.J., et al., *Reactive boiling of cellulose for integrated catalysis through an intermediate liquid.* Green Chemistry, 2009. **11**(10): p. 1555-1561.

18. Bridgwater, A.V., *The production of biofuels and renewable chemicals by fast pyrolysis of biomass.* International Journal of Global Energy Issues, 2007. **27**(2): p. 160-203.

19. Mohan, D., C.U. Pittman, Jr., and P.H. Steele, *Pyrolysis of wood/biomass for bio-oil: A critical review.* Energy & Fuels, 2006. **20**(3): p. 848-889.

20. Demirbas, A. and G. Arin, *An overview of Biomass pyrolysis.* Energy Sources, 2002. **24**(5): p. 471-482.

21. Bridgwater, A.V., D. Meier, and D. Radlein, *An overview of fast pyrolysis of biomass.* Organic Geochemistry, 1999. **30**(12): p. 1479-1493.

22. Mettler, M.S., D.G. Vlachos, and P.J. Dauenhauer, *Top ten fundamental challenges of biomass pyrolysis for biofuels.* Energy & Environmental Science, 2012. **5**(7): p. 7797-7809.

23. Srinivasan, V., et al., *Catalytic Pyrolysis of Torrefied Biomass for Hydrocarbons Production.* Energy & Fuels, 2012. **26**(12): p. 7347-7353.

24. Coates, J., *Interpretation of Infrared Spectra, A Practical Approach*, in *Encyclopedia of Analytical Chemistry*. 2000, John Wiley and Sons Ltd: Chichester. p. 10815-10837.

25. Smith, C., and Brian, *Fundamentals of Fourier Transform Infrared Spectroscopy*. Second ed. 2011: Taylor and Francis Group.

26. Siengchum, T., M. Isenberg, and S.S.C. Chuang, *Fast pyrolysis of coconut biomass - An FTIR study.* Fuel, 2013. **105**: p. 559-565.

27. Bassilakis, R., R.M. Carangelo, and M.A. Wojtowicz, *TG-FTIR analysis of biomass pyrolysis.* Fuel, 2001. **80**(12): p. 1765-1786.

28. Feng, J., W.Y. Li, and K.C. Xie, *Thermal decomposition behaviors of lignite by pyrolysis-FTIR.* Energy Sources Part a-Recovery Utilization and Environmental Effects, 2006. **28**(1-3): p. 167-175.

29. Feng, J., Q. YuHong, and A.E.S. Green, *Analytical model of corn cob Pyroprobe-FTIR data.* Biomass & Bioenergy, 2006. **30**(5): p. 486-492.

30. Li, S., et al., *Real-time evolved gas analysis by FTIR method: an experimental study of cellulose pyrolysis.* Fuel, 2001. **80**(12): p. 1809-1817.

31. Roy, S., et al., *Temperature measurements in reacting flows by time-resolved femtosecond coherent anti-Stokes Raman scattering (fs-CARS) spectroscopy.* Optics Communications, 2008. **281**(2): p. 319-325.

32. Roy, S., J.R. Gord, and A.K. Patnaik, *Recent advances in coherent anti-Stokes Raman scattering spectroscopy: Fundamental developments and applications in reacting flows.* Progress in Energy and Combustion Science, 2010. **36**(2): p. 280-306.

33. Miller, J., *Hybrid femtosecond/picosecond coherent anti-Stokes Raman scatteringfor gas-phase temperature measurements*, in *Mechanical Engineering*. 2012, Iowa State University. p. 187.

34. Engel, S.R., et al., *Hybrid femtosecond/picosecond coherent anti-Stokes Raman scattering for high-speed CH4/N-2 measurements in binary gas mixtures.* Pharmacotherapy, 2013. **33**(10): p. 1336-1343.

35. Richardson, D.R., et al., *Theoretical modeling of single-laser-shot, chirped-probe-pulse femtosecond coherent anti-Stokes Raman scattering thermometry.* Applied Physics B-Lasers and Optics, 2011. **104**(3): p. 699-714.

36. Miller, J.D., et al., *Hybrid femtosecond/picosecond coherent anti-Stokes Raman scattering for high-speed gas-phase thermometry.* Optics Letters, 2010. **35**(14): p. 2430-2432.

37. Miller, J.D., et al., *Single-shot gas-phase thermometry using pure-rotational hybrid femtosecond/picosecond coherent anti-Stokes Raman scattering.* Optics Express, 2011. **19**(16): p. 15627-15640.

38. Patwardhan, P.R., et al., *Product distribution from fast pyrolysis of glucose-based carbohydrates.* Journal of Analytical and Applied Pyrolysis, 2009. **86**(2): p. 323-330.

39. Ronsse, F., et al., *Optimization of platinum filament micropyrolyzer for studying primary decomposition in cellulose pyrolysis.* Journal of Analytical and Applied Pyrolysis, 2012. **95**: p. 247-256.

40. Dayton, D.C., *Laminar Entrained Flow Reactor for Biomass ThermochemicalConversion Studies*. 2000, National Energy Renewable Laboratory. p. 23.

41. Dupont, C., et al., *Biomass pyrolysis experiments in an analytical entrained flow reactor between 1073 K and 1273 K.* Fuel, 2008. **87**(7): p. 1155-1164.

42. Xiu, S.N., et al., *Devolatilization characteristics of biomass at flash heating rate.* Fuel, 2006. **85**(5-6): p. 664-670.

43. Visentin, V., F. Piva, and P. Canu, *Experimental study of cellulose fast pyrolysis in a flow reactor.* Industrial & Engineering Chemistry Research, 2002. **41**(20): p. 4965-4975.

44. Klee, M. *GC Solutions #11: The Flame Ionization Dector*.

45. Holm, T., *Aspects of the mechanism of the flame ionization detector.* Journal of Chromatography A, 1999. **842**(1-2): p. 221-227.

46. Patwardhan, P.R., R.C. Brown, and B.H. Shanks, *Product Distribution from the Fast Pyrolysis of Hemicellulose.* Chemsuschem, 2011. **4**(5): p. 636-643.

47. Patwardhan, P.R., R.C. Brown, and B.H. Shanks, *Understanding the Fast Pyrolysis of Lignin.* Chemsuschem, 2011. **4**(11): p. 1629-1636.

48. Wu, S., et al., *TG-FTIR and Py-GC-MS analysis of a model compound of cellulose - glyceraldehyde.* Journal of Analytical and Applied Pyrolysis, 2013. **101**: p. 79-85.

49. Patwardhan, P., *Understanding the product distribution from biomass fast pyrolysis*, in *Chemical Engineering*. 2010, Iowa State University: Iowa State University. p. 153.

50. Daimay, L.-V., et al., *The Handbook of Infrared and Raman Characteristic*. 1991, Boston: Academic Press Inc.

51. Wang, S., et al., *Mechanism Study on Cellulose Pyrolysis using Thermogravimetric Analysis Coupled with Infrared Spectroscopy.* Frontiers of Energy and Power Engineering in China, 2007. **1**(4): p. 413-419.

52. Zhang, Z., *Fast Pyrolysis behavior of different celluloses and lignocellulosic biopolymer interaction during fast pyrolysis*, in *Chemical Engineering*. 2012, Iowa State University. p. 86.